Biosensors and Bioelectronics 76 (2016) 213–233

Contents lists available at ScienceDirect

Biosensors and Bioelectronics

journal homepage: www.elsevier.com/locate/bios

Recent advances in lab-on-a-chip for biosensing applications

Josiane P. Lafleur, Alexander Jönsson, Silja Senkbeil, Jörg P. Kutter*

Department of Pharmacy, University of Copenhagen, Copenhagen, Denmark

ARTICLE INFO

Article history:
Received 18 June 2015
Received in revised form
31 July 2015
Accepted 3 August 2015
Available online 13 August 2015

Keywords:
Biosensors
Microfluidics
Lab-on-a-chip
Electrochemical
Optical
Micromechanical
Review

ABSTRACT

The marriage of highly sensitive biosensor designs with the versatility in sample handling and fluidic manipulation offered by lab-on-a-chip systems promises to yield powerful tools for analytical and, in particular, diagnostic applications. The field where these two technologies meet is rapidly and almost violently developing. Yet, solutions where the full potentials are being exploited are still surprisingly rare. In the context of this review, sensor designs are often fairly advanced, whereas the lab-on-a-chip aspect is still rather simplistic in many cases, albeit already offering significant improvements to existing methods. Recent examples, showing a staggering variety of lab-on-a-chip systems for biosensing applications, are presented, tabularized for overview, and briefly discussed.

1. Introduction

The field of biosensors is vast and complex to begin with. If you add to it the possibility to combine a biosensing element with microfluidic sample handling capabilities, the number of realizations described in the literature and being the subject of current research efforts becomes almost, if not quite, astronomical. One reason for the complexity of the field of biosensors is that the term itself is often rather loosely defined, or, at least, means different things to different people. In fact, it is often (erroneously) considered that a biosensor is a device that senses the presence (and typically the quantity) of a biomolecule (such as a protein or a DNA strand) or perhaps a cell. However, the guidelines for this journal (Biosensors and Bioelectronics) stipulate that a biosensor needs to incorporate a biological, biologically derived or biomimetic recognition element in close integration with a transducing element (http://www.journals.elsevier.com/biosensors-and-bioelectronics/). In other words, there has to be a biological response (which can be triggered by any type of analyte), which then is converted to an electrical signal by means of an optical, electrochemical, thermometric, piezoelectric, magnetic or micromechanical transducer. In this review, we have attempted to adhere to this definition in order to bring down the inherent complexity. Other authors have also commented on the ambiguity of the term "biosensor" and in particular the confusion of the terms "sensor" and "probe" (Borisov and Wolfbeis, 2008).

It is beneficial for a number of reasons to combine biosensor designs with microfluidic circuits to improve the overall performance of the sensing system. The main motivation here is certainly to improve transport of analyte from the sample volume to the biorecognition element, in particular for surface-bound sensing elements. The reduced dimensions and volumes in microfluidic channels allow first of all to work with much less sample than what otherwise might be used, making analysis on drops of blood or even the contents of single cells possible. But, more importantly, the reduced distances for analyte molecules to diffuse to the biorecognition elements immediately yield a great gain in response time, significantly improving conditions for diffusion-limited processes. Moreover, specially designed channels can further improve convective transport to the sensor surfaces by, e.g., including flow focusing or helical flows (Lynn et al., 2015; Lynn and Homola, 2015). Expanding from pure microfluidics to more fully developed lab-on-a-chip solutions, entire sample preparation procedures can be incorporated prior to the sensing, such as separation, enrichment, and labeling, to name but a few. All of these pre-sensing steps can improve the actual detection step by removing interfering species or by increasing the concentration of analyte in the detection volume. When scanning the literature, one finds indeed a wealth of papers that utilize microfluidics in order to transport sample containing the analyte(s) of interest, but it is somewhat surprising that most of the realizations are very basic, often only comprising a single channel with an inlet and an outlet and thus allowing not much more than to flush sample across the

* Corresponding author.
E-mail address: jorg.kutter@sund.ku.dk (J.P. Kutter).

http://dx.doi.org/10.1016/j.bios.2015.08.003
0956-5663/

Table 1
Summary of recent advances in enzyme-based electrochemical sensors in microfluidic applications.

Analyte	Biological recognition element	LOD and/or Linear range	Microfluidic chip features	Reference
Amperometry				
Glucose	Glucose oxidase immobilized on paper	n.a.	PDMS flow cell	Tan et al. (2012)
Adenosine- 5′-triphosphate (ATP)	Glycerol kinase and glycerol-3-phosphate oxidase	3.9 μM	PDMS chip, droplet based operation	Itoh et al. (2012)
Phenol	Tyrosinase immobilized on graphene micropillars	50 nM	PDMS flow channel with 3D micropillars to enhance surface area for enzyme immobilization	Liu et al. (2013)
Ebstein-Barr Virus (EBV)	Anti-EBV viral capsid antigen	n.a.	Meandering channel layout for immobilization and hydrophobic stop to prevent liquid leakage into the sensing area, material: dry film photoresist, Vacrel® 8100 on polyamide substrate	Horak et al. (2014)
Acetylthiocholine	Acetylcholinesterase enzyme immobilized on PMMA	measurement range 0.1–0.9 mM	Microfluidic chip (PMMA) with enzyme chamber and reaction chamber	Yoon et al. (2014)
Glucose	Glucose oxidase immobilized on PMMA	0.5 μmol L^{-1}	Flow channel (PMMA) with additional off channel detection	Cerqueira et al. (2014)
Glucose, glutamine, glutamate	Glucose oxidase, glutamate oxidase and glutaminase immobilized on platinum thin-film electrodes	0.05–20 mM (glucose) 0.05–10 mM (glutamate) 0.1–20 mM (glutamine)	SU-8 flow channel with simultaneous determination of three analytes	Bäcker et al. (2013)
Glucose	Glucose oxidase	0.05 mM/0.2–43.5 mM	Droplet based microfluidic chip with electrochemical detection inside droplets; the microfluidic electrochemical sensor was tested with human blood serum samples	Gu et al. (2014)
Chronoamperometry				
MicroRNA	Biotinylated DNA capture probes immobilized on streptavidin-coated paramagnetic beads; Enzymatic reaction catalyzed with streptavidin -alkaline phosphatase conjugate	7 pmol L^{-1}/0–1 nmol L^{-1}	Gravi-Cell (DiagnoSwiss, Monthey, Switzerland)	Bettazzi et al. (2013)
Glucose	Glucose oxidase	Measurement range: 0.5–50 mM	PDMS channel, including four separate microreactors that feature prolonged blood analysis, automated background subtraction, autocalibration	Picher et al. (2013)
Cyclic voltammetry				
Extracellular H_2O_2 secreted from hepatocytes	Horseradish peroxidase entrapped in PEG-hydrogel	0.2–100 μM	PDMS flow channel	Matharu et al. (2013)
Cholesterol	Cholesterol esterase and cholesterol oxidase functionalized chitosan/anatase titanium dioxide nanoparticles	0.65–10.3 mM	PDMS flow channel	Ali et al. (2013)
Clenbuterol (CLB) in bovine hair sample	Anti-CLB antibodies immobilized on magnetic microparticles	0.008 ng mL^{-1}/0.027–800 ng mL^{-1}	PMMA microfluidic chip with integrated screen printed electrodes; competitive immunoassay with alkaline phosphatase	Regiart et al. (2013)
Redox cycling				
Mouse IgG and human cardiac troponin I (cTnI)	Antimouse IgG/anti-cTnI and alkaline phosphatase immobilized on 3D interdigitated indium tin oxide electrodes	10 fg mL^{-1} (mouse IgG) 100 fg mL^{-1} (cTnI)	Microfluidic glass chip with interdigitated electrodes on bottom and ceiling of channel, which is channel formed by adhesive tape	Han et al. (2014)
Impedance spectroscopy				
Cholesterol	Cholesterol esterase (ChEt) and cholesterol oxidase (ChOx) immobilized on chitosan/anatase titanium dioxide nanoparticles electrode	0.2 mg dL^{-1}/2–500 mg dL^{-1}	Three PDMS flow channels	Ali et al. (2014)
Cyclic voltammetry and amperometry				
Glucose	Glucose oxidase	0.29 mM	PDMS centrifugal microfluidic device featuring a reservoir, a mixing chamber, a spiral channel, a carbon-paste electrode detector and a waste reservoir	Rattanarat et al. (2015)

sensor surface, or to bring two or more reagents together. Only rarely do we find more advanced solutions or systems where several (other) functionalities are integrated to come closer to the goals of the lab-on-a-chip philosophy. The reasons for sticking with a simple microfluidic cell can be manifold and differ from case to case, ranging from putting an emphasis on the biosensor design to a deliberate reduction of complexity and thus sacrificing sophistication for the sake of reliable operation. However, it is dangerous to view the microfluidic channel (and its design) as a separate part, while it is in fact an integral part of what makes the entire biosensing system work as intended. Some of the most important design considerations for combining (planar) sensors with microfluidic systems are laid out and explained in a paper by Squires et al. (2008). Here, the interplay between channel dimensions, sensor dimensions, flow velocities, diffusional transport, advective transport and reaction rate are explored and the consequences of a bad design on the overall performance of the sensor system are investigated. Undoubtedly, there are a number of examples in the literature where microfluidic (bio)sensors underperform on account of a flawed design or because they are operated under sub-optimum conditions. Serendipitous cases of sensor designs performing better than expected are further indications that a better theoretical understanding and improved models are still lacking.

For this review article, we have collected examples from the literature from 2012 onwards describing sensors utilizing a biorecognition element according to the definition given above. We have attempted to achieve a rough structure by sorting the described systems according to the used transduction principle, as these are just slightly less numerous and less diverse than the number of biorecognition elements exploited and investigated. The latter include, among others, enzymes, antibodies, DNA strands, aptamers, peptides, receptors, bacteria and other cells, and either direct or indirect reactions and interactions of these with the analyte(s) of interest. The complexity of the matter combined with the ingenuity of the researchers in finding novel approaches makes it almost impossible to avoid inclusion of "borderline" cases on the one hand, and missing some papers entirely, on the other hand. There are, in particular, many cases where an enzyme is used to turn over a substrate and where the product of this enzymatic reaction is then detected. Such instances are clearly in a "greyzone" when held against the definition mentioned earlier, especially when the enzyme is added like a reagent and not really part of the sensor as such. We hope that the readers will find this review nonetheless a great resource and a starting point for further explorations. For a quick overview, the main facts and findings from the cited papers are summarized in several tables. The readers are also referred to recent related reviews that might be of interest (Bunyakul and Baeumner, 2014; Ferrier et al., 2015; Ge et al., 2014; Holzinger et al., 2014; Jiang et al., 2014; Kelley et al., 2014; Muzyka, 2014; Reenen et al., 2014; Rocha-Santos, 2014; Sang et al., 2014).

2. Microfluidic biosensors based on electrochemical transduction

Electrochemical detection is generally based on the interplay between electricity and chemistry and in terms of biosensors on the signal generation via a biochemical recognition event, which can be measured as a change in current, voltage, conductance or impedance (Wang, 2006). Typically, in biosensors the electrochemical transducer measures a potential shift (potentiometric) or a change in current triggered by a biorecognition (immobilization) event under a fixed (amperometric) or variable potential (voltammetric) (Grieshaber et al., 2008). Electrogenerated chemiluminescence and photoelectrochemical bioanalysis are not covered here, but interested readers are referred to recent reviews in the field (Muzyka, 2014; Zhao et al., 2014).

Electrochemical biosensors are generally very sensitive, have a rapid response and are often designed to be selective towards the analyte in question (Han et al., 2013). Inherently, they are not dependent on the optical path length or the optical properties of the material. Easily miniaturized and incorporated into microfluidic systems, they can often offer a less expensive read-out than optical systems.

3. Enzyme based detection

Functionalization of electrodes with enzymes can make use of their ability to selectively catalyze chemical reactions. The generated or consumed electroactive species can be detected via a change in current. For example, enzyme based electrodes have been intensively used for glucose determination (Ispas et al., 2012; Kimmel et al., 2012; Liu et al., 2012c). Recent advances in enzyme-based biosensor developments for microfluidic applications are summarized in Table 1.

4. Affinity based detection

Electrochemical biosensors are very suitable for detecting affinity based biorecognition events and an electrochemical signal can be recorded from such a binding event. Amperometric detection is the most common method of detection, but electrochemical impedance spectroscopy (EIS) is also often applied in the field of affinity-based biosensors. EIS offers the advantage of label free detection of binding events and is a technique to determine the complex electrical resistance of a system (Lisdat and Schäfer, 2008). Several electrochemical biosensor types, including immunoassays, DNA hybridization and signal switching aptamer sensors have been studied and found application in microfluidic systems. Real samples often have to be treated before they can be introduced to the biosensor (Bunyakul and Baeumner, 2014), but due to their specific binding capabilities, affinity based biosensors are capable of handling complex sample matrixes and samples. Real milk (Daprà et al., 2013), stool (Bunyakul et al., 2014), poultry meat (Morant-Miñana and Elizalde, 2015) and blood/serum (Ferguson et al., 2013; He et al., 2013; Kim et al., 2013b; Seia et al., 2014) have all been analyzed with microfluidic electrochemical affinity sensors. Miniaturization, and integration into microfluidic devices, often leads to faster analysis times and to efficient collection of electroactive species due to improved transport ("non-planar diffusion") and thus a higher sensitivity of the sensor (Ghosh Dastider et al., 2015; Hervás et al., 2012; Ben-Yoav et al., 2012; Zuzuarregui et al., 2014).

For example, (Seia et al., 2014) could demonstrate that an electrochemical immunosensor combined with a microfluidic chip reduces the analysis time by a factor of 3.8 for thyrotropin (TSH) compared to an ELISA test, and also improves the sensitivity. Recent advances in affinity-based biosensor developments for microfluidic applications are summarized in Table 2.

5. Microfluidic applications highlights

Most articles screened for this review focus on the sensor development and use simple microfluidic concepts such as flow cells (Seenivasan et al., 2015; Song et al., 2013; Wang et al., 2014b; Zitka et al., 2013; Zuzuarregui et al., 2014) or (PDMS) flow channels, some with a full lab-on-chip integration in mind (Morant-Miñana

and Elizalde, 2015; Vabbina et al., 2015). The following biosensors are examples of more complex platforms towards integrated lab-on-a-chip sensors:

Ferguson et al. (2013) implemented a vertical flow diffusion filter (CDF) for the detection of doxorubicin, a chemotherapeutic drug, in whole blood samples. Within the CDF, smaller target molecules diffuse to the electrode where they are detected by a signal switching aptamer sensor. The device had a LOD of 10 nM and a dynamic range from 0.01–10 μM spanning the therapeutic range of the drug.

Shin et al. (2013) have utilized a microfluidic PDMS flow channel on Au structured glass for the detection of cell-secreted metalloproteinase (MMP9), a key reporter in many pathological processes. The group engineered a specific methylene blue (MB) conjugated peptide with end-terminal cysteine for self-assembled monolayer (SAM) immobilization on Au electrodes. MB is, besides anthraquinone (AQ) and $(Fe(CN)_6)^{3-/4-}$ (FCN), a commonly used redox reporter. Monocyte cells were immobilized next to the electrode via antibody capture in PEG hydrogel. Proteolytic cleavage of the MB conjugated peptide causes a significant drop in amperometric detection. A detection limit of 60 pM and a linear range extending to 50 nM was reported.

Liu et al. (2012b) used a similar microfluidic cell capture approach to simultaneously detect the cytokines interferon gamma (IFN-γ) and tumor necrosis factor alpha (TNF-α) secreted from human T-cells and monocytic cells. Instead of the proteolytic cleavage, they chose the simpler and more specific dual-aptamer approach, using two cytokine specific aptamers, labeled with MB and AQ. Upon analyte binding, the aptamer hairpin unfolds and the conformational change decreases the electron transfer, a detectable amperometric drop for the respective redox mediator. The sensor is highly specific with a LOD in the low ng mL^{-1} range for both cytokines.

Polydimethylsiloxane (PDMS) is a soft and deformable elastomer and has been used extensively for micro valve applications. Matharu et al. (2014) have adopted this approach and used a three-layer microfluidic device, comprising an Au electrode glass bottom layer, a microfluidic channel with microcups and a PDMS control or actuation channel (Fig. 1). During cell seeding into the microfluidic channel the disk-shaped microcups are pressed onto the electrode surface by means of the actuation channel. Upon microcup release, transforming growth factor-beta 1 (TGF-β1) released from the seeded cells can be amperometrically detected with a signal switching aptamer sensor at LODs of 1 ng mL^{-1}.

A more complex and fully integrated microfluidic devices was described by Kim et al. (2013b) comprising a centrifugal microfluidic disk device for the detection of C-reactive protein (CRP), a biomarker for cardiovascular disease, via horseradish peroxidase (HRP) catalyzed 5-thio-2-nitrobenzoic acid (TNB) redox cycling. The device integrates several loading, washing and reaction steps with a sample to answer time of approximately 20 min and 21.3 pg mL^{-1} LOD, a 4-fold increase to a stationary (no flow) electrochemical reference measurement.

Ben-Yoav et al. (2015) presented a lab-on-a-chip device for electrochemical analysis of DNA hybridization events. A new dual layer microfluidic valved manipulation system (Fig. 2) integrated into the device provides controlled and automated capabilities for high throughput analysis. The device yields semilogarithmic dose response and enables a theoretical detection limit of 1 nM of complementary ssDNA target.

Itoh et al. (2012) presented a droplet-based microfluidic device constructed for on-site determination of fish freshness (Fig. 3). The droplet-based system allows mixing and metering of extracts, enzymes and buffers with a sensing region located downstream. The data obtained for jack mackerel extracts correlated well with those obtained by high-performance liquid chromatography (HPLC).

6. Microfluidic biosensors based on optical transduction

Due to the ease of interfacing microfluidic devices with the conventional optical detection instruments commonly found in laboratories (inverted fluorescence microscopes, digital CCD cameras, simple LEDs and photodiodes set-ups, and even smartphones), optical detection is ubiquitous in microfluidic applications. Innovations in optical microfluidic technologies for point-of-care diagnostics have been reviewed by Myers and Lee (2008). Recent review articles have focused more specifically on label-free optical biosensing platforms (Estevez et al., 2014; Fan et al., 2008; Wang et al., 2013b) while biosensors based on measurement of absorbance, reflectance and fluorescence have been reviewed extensively by Borisov and Wolfbeis (2008).

7. Fluorescence-based biosensors

Fluorescence-based biosensors are by far the most prevalent type of biosensor encountered in microfluidic applications thanks to their ease of implementation. They benefit from very low detection limits, high selectivity and the wide array of fluorescence labels available for tagging biomolecules. However, quantitative analysis can be hindered by the auto-fluorescence generated by the microfluidic chip material in the case of polymeric devices. Recent advances in fluorescence-based biosensors in microfluidic applications are summarized in Table 3.

8. Label-free and other non-fluorescence-based optical biosensors

In evanescence wave-based biosensors, the probing light is concentrated in an evanescent field, within a few hundred nanometers of the sensor surface. Evanescence-based biosensors can be used in fluorescence or label-free measurements. In fluorescence measurements, the light transmitted can be used to excite fluorescently labeled analytes immobilized at the surface of the waveguide. Only the fluorescent labels located in close vicinity of the waveguide surface are excited, minimizing background fluorescence from the bulk solution. Evanescent wave fluorescence biosensors are reviewed by Taitt et al. (2005). Evanescent wave biosensors can also be used as a label-free technique. Indeed, these biosensors are capable of detecting the refractive index (RI) change induced by the analyte binding to their surface. Since the detection signal does not scale down with the sample volume (Fan et al., 2008), these sensors are especially attractive for use in microfluidic applications.

Surface Plasmon Resonance (SPR) refers to the resonant oscillation that occurs at the interface of two media with dielectric constants of opposite signs, such as a metal (gold or silver) and a dielectric material stimulated by incident light (Fan et al., 2008). Localized SPR (LSPR), on the other hand, refers to the collective resonant oscillation of conduction electrons at the surface of a metal nanoparticle under the perturbation of incident light (Myers and Lee, 2008). Conventional SPR sensing a prism, waveguide, fiber optic or grating coupling (Fan et al., 2008) to excite propagating plasmons on the surface of the gold or silver surface. On the other hand, LSPR sensing requires no special coupling instrumentation and is typically performed with a white light source (Myers and Lee, 2008). In both cases, when the analyte of interest binds to the surface of the sensor, a marked shift in resonance wavelength is observed. SPR and LSPR are near-field phenomena

Table 2
Summary of recent advances in affinity-based electrochemical sensors in microfluidic applications.

Analyte	Biological recognition element	LOD and/or Linear range	Microfluidic chip features	Reference
Impedance spectroscopy				
ssDNA	ssDNA modified Au electrodes	3.8 nM	PDMS flow channel with improved analysis due to dominant diffusion in microchannel	Ben-Yoav et al. (2012)
Ampicillin kanamycin A	ssDNA aptamer immobilized on tosylate doped poly(3,4-ethylenedioxythiophene) PEDOT-OH:TsO	100 pM (ampicillin) 10 nM (kanamycin A)	COC flow channel with detection in real milk samples	Daprà et al. (2013)
dsDNA	ssDNA modified nanoporous alumina membrane	n.a.	PDMS flow channel with integrated membrane;signal enhancement with Ag modified AuNP	Ye et al. (2013)
Liposomes HIV	Antibody functionalized Au electrode	n.a. (HIV) 1000 liposomes μL^{-1}	PDMS flow channel; demonstrates liposome ion-release impedance spectroscopy for virus detection	Damhorst et al. (2013)
Thrombin	Aptamer modified magnetic beads	0.01–10 nM,	PDMS flow cell	Wang et al. (2014b)
Salmonella typhimurium	Monoclonal anti-salmonella antibodies immobilized on the surface of an Au electrode	3000 CFU mL^{-1}	PDMS flow channel;integration into microfluidic channel improved detection limit	Ghosh Dastider et al. (2015)
Lipoprotein LDL	Anti-apolipoprotein B immobilized on CNT-NiO modified ITO electrode	6.3 $\mu g\ ml^{-1}$ (CNT-NiO)	PDMS flow channel	Ali et al. (2015)
ssDNA	ssDNA self-assembled on Au electrode	1 nM	PDMS microfluidic assay with 9 sensors and PDMS valves.	Ben-Yoav et al. (2015)
Square wave voltammetry (SWV)				
Cell secreted metalloproteinase (MMP9)	Specific peptide immobilized on Au electrode	60 pM to 50 nM	Flow channel with detection cell	Shin et al. (2013)
Transforming growth factor-beta 1 (TGF-β1)	Aptamer modified Au electrode	1–250 ng mL^{-1}	Glass-PDMS device with flow channel and PDMS valving mechanism to avoid cell-electrode attachment	Matharu et al. (2014)
Interferon gamma (IFN- γ) and tumor necrosis factor alpha (TNF-α)	Aptamers immobilized on Au electrode	6.35 ng mL^{-1} (IFN-γ) 5.46 ng mL^{-1} (TNF-α)	PDMS flow channel with PEG hydrogel Au electrode array for cell capture	Liu et al. (2012b)
Campylobacter spp	DNA thiolated probe modified Au electrode	90 pM/1–25 nM	COP microfluidic cartridge, tested with poultry meat samples	Morant-Miñana and Elizalde (2015)
Cell secreted cytokines: TNF-a and INF-y	Aptamers immobilized on Au electrode	10 –100 ng mL^{-1} (0.58–5.8 nM) (TNF-α) 0.06–10 nM (INF-γ)	Cells were infused into the PDMS microfluidic device and stimulated to commence cytokine production; dual detection of two cell-secreted cytokines at the same electrode	Liu et al. (2015)
Doxorubicin (chemotherapeutic) and kanamycin (antibiotic)	Aptamer probe immobilized on Au electrode	10 nM/0.01–10 μM	Flow diffusion filter; dynamic range spanning the drug's therapeutic range	Ferguson et al. (2013)
Amperometry				
Vasopressin	Aptamers immobilized on carbon nanotubes	43 pM	PDMS flow channel	He et al. (2013)
TSH thyrotropin	Anti-TSH antibody immobilized on ZnO nanobeads	0.00087 μUI mL^{-1}	Microfluidic glass chip; cross-shaped channel layout with 3 inlets for washing buffer, immobilization molecules and sample	Seia et al. (2014)
C-reactive protein (CRP)	Antibody coated polystyrene beads	4.9 pg mL^{-1}	Centrifugal microfluidic platform including sample loading, washing and reaction steps; sample to answer in less than 20 min	Kim et al. (2013b)
Myeloperoxidase (MPO), (cardiovascular biomarker)	Anti-MPO coated magnetic beads	0.200 ng mL^{-1} (MPO Active) and 0.004 ng mL^{-1} (MPO total)	COP microfluidic chip; amperometric steady state current under flow (MPO activ) and peak current (MPO total) under stopped flow	Moral-Vico et al. (2015)
ssDNA (cyanobacteria nucleic acids)	ssDNA capture probe immobilized on Au electrode	6 pM	On-line hybridization leads to short assay time (25 min)	Ölcer et al. (2015)
Differential pulse voltammetry (DPV)				
Lactoferrin (LF)	Goat anti-LF antibody modified paramagnetic beads	0.1 $\mu g\ mL^{-1}$ 0.195–100 $\mu g\ mL^{-1}$	Commercially available flow cell (CH Instrument Inc., TX, USA)	Zitka et al. (2013)

Table 2 (*continued*)

Analyte	Biological recognition element	LOD and/or Linear range	Microfluidic chip features	Reference
ssDNA	ssDNA modified MWCNTs	n.a. (detection of 1.36 μM and 13.6 μM)	PDMS flow channel	Kim et al. (2013a)
Cyclic voltammetry				
Cortisol	Anti-cortisol antibodies immobilized on Au electrodes	10 pg mL^{-1}/10 pM to 100 nM	Flow channel made of low temperature co-fired ceramic	Vasudev et al. (2013)
Cholera toxin (CT) subunit B	Capture: anti-CTB antibody modified magnetic beads	31.7 ng mL^{-1}	PDMS flow cell; detection in stool samples	Bunyakul et al. (2014)
Endotoxin	Capture: synthetic peptide immobilized on Au electrode	21.8 pg mL^{-1} to 1 ng mL^{-1}	Silicon based sensor embedded in methacrylate flow cell	Zuzuarregui et al. (2014)
Circulating tumor cells (CTC)	MC1R-antibodies immobilized in amino-functionalized silica nanoparticles (n-SiNPs)-polypyrrole (PPy) nanocomposite modified on working electrode surface of screen-printed electrode (SPE)	20 cells mL^{-1}	Flow cell	Seenivasan et al. (2015)
Cortisol	Anti-cortisol antibody (Anti-Cab) immobilized on ZnO nanostructures	1 pM	Potential for microfluidic integration; LOD in physiological range and 100 times better then conventional ELISA assay	Vabbina et al. (2015)
Redox Cycling				
Secreted alkaline phosphatase (SEAP)	Anti-SEAP modified sensor points (microwells)	<5 μM	256 microwell array for single cell analysis	Şen et al. (2012)
Miscellaneous				
Adenosine	Aptamer functionalized polystyrene microbeads trapped within the paper fluidic channel	11.8 μM	Origami paper analytical device laminated in plastic; the transducer is based on a concentration cell, which acts as a battery to charge a capacitor that is subsequently read-out using a digital multimeter	Liu et al. (2012a)

*Abbreviations: Limit of detection (LOD), polydimethylsiloxane (PDMS), polymethylmethacylate (PMMA), cyclic olefin copolymer (COC), single-stranded DNA (ssDNA), double-stranded DNA (dsDNA), gold nanoparticle (AuNP), (Multi-walled) carbon nanotube ((MW)CNT).

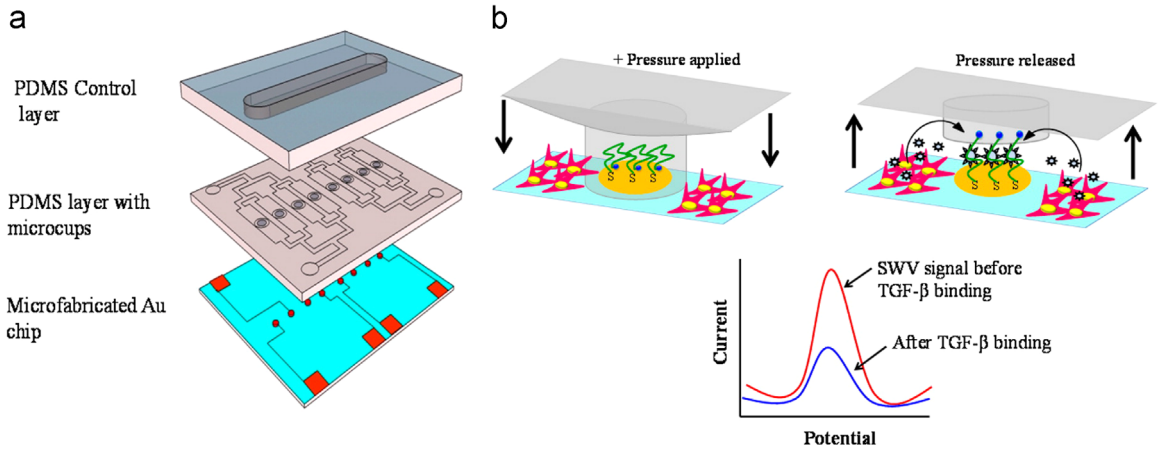

Fig. 1. (A) Microfluidic device composed of three layers: a glass slide with micropatterned Au electrodes, a PDMS layer with fluid channels and microcups, and another PDMS layer for controlling the microcups. (B) Diagram showing actuation of microcups to protect electrodes during collagen coating and cell seeding into the channel. Reprinted with permission from Matharu et al. (2014).

and therefore minimize background. Estevez et al. (2014) compare the state-of-the-art of refractometric SPR and novel LSPR biosensors. Interferometric sensing assesses binding events by measuring the phase shift between two optical paths, one functionalized with a biological recognition element, which can bind the analyte of interest, and a reference (unfunctionalized) path. The resulting interference pattern can be used to measure binding events in the functionalized microchannel. Although absorbance spectrometry is a standard technique employed in most biochemical and analytical chemistry laboratories, its downscaling suffers from the short absorbance pathlengths available in microfluidic devices. However, when quantification at low levels is not necessary, colorimetric tests are easily implemented on microfluidic platforms. Chemical luminescence includes chemiluminescence, bioluminescence, and electrogenerated chemiluminescence. Chemical luminescence is a method of choice for microfluidic applications due to the absence of an excitation source and the resulting low backgrounds. Chemical luminescence-based lab-on-chip and microfluidic platforms for bioanalysis have previously been reviewed by Mirasoli et al. (2012).

Finally, many bead-based assays rely on the measurement of changes in scattered light due to the agglomeration of the micro- or nanoparticles. Recent advances in label-free optical biosensors and other non-fluorescence-based biosensors in microfluidic devices are summarized in Table 4.

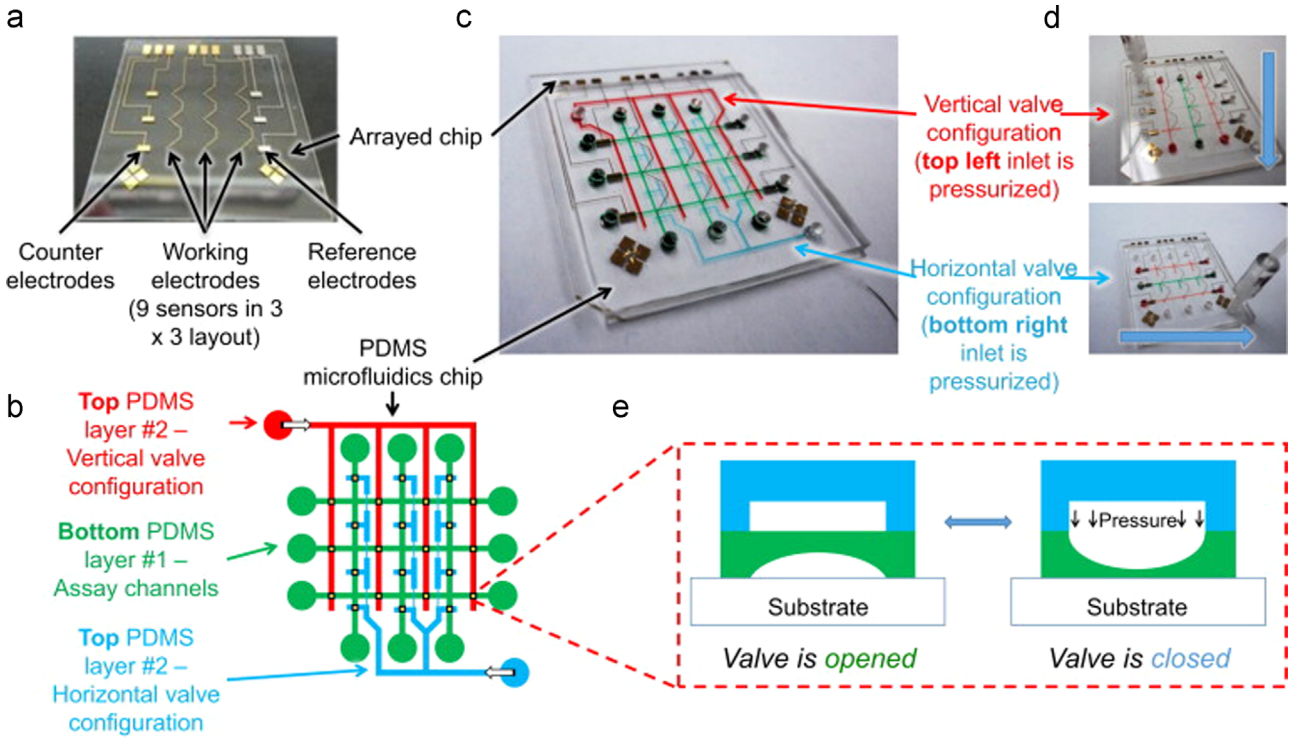

Fig. 2. Microfluidic valved arrayed electrochemical LOC. (A) Photographs of the fabricated arrayed electrochemical chip (3.5 cm × 4 cm). (B) Layout of the top valve configuration (blue or red) and the bottom assay (green) channels. (C) A photograph of the entire assembled device. Assay channels are filled with green dye, and valve channels are filled with either blue or red dye for horizontal or vertical assay channels orientation, respectively. (D) Photographs of the vertical (top) and the horizontal (bottom) valve configurations with the resulted assay channels orientation filled with red and green dyes. Thick arrows indicate fluid flow direction. (E) Schematic demonstrating valve actuation using hydraulic channel to pinch off the microfluidic assay channel below. Left – valve is opened when no pressure is applied. Right – valve is closed upon pressure application. Reprinted with permission from Ben-Yoav et al. (2015).

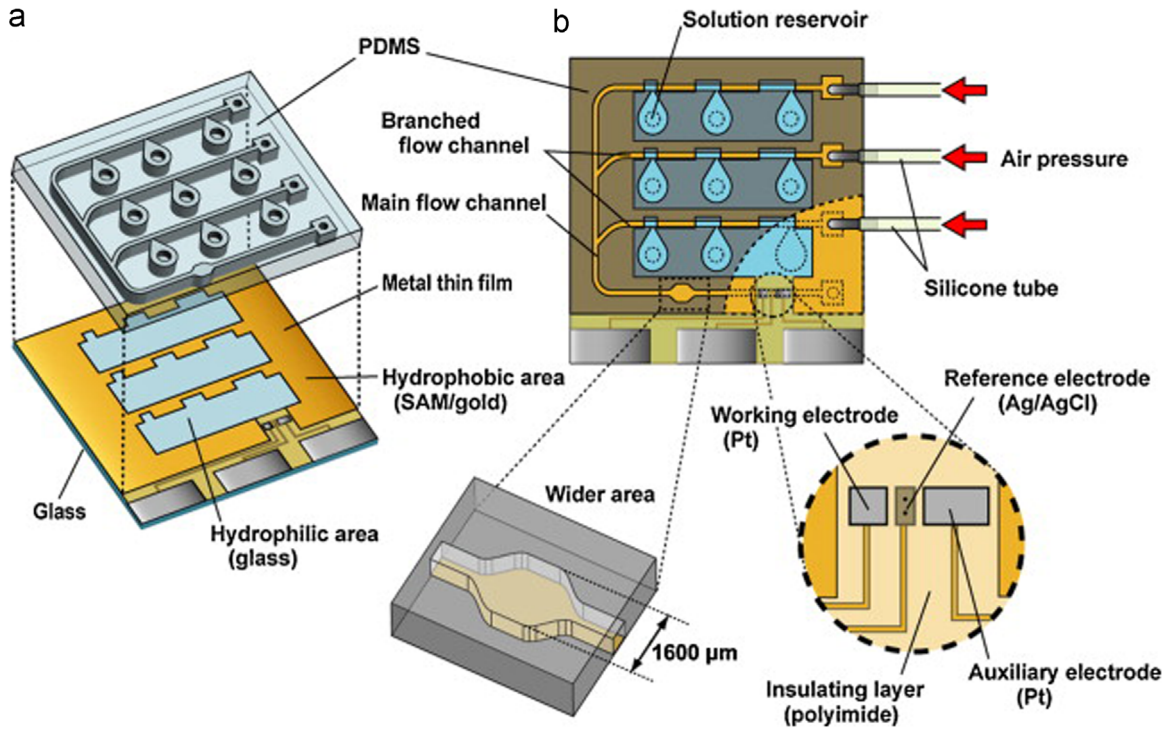

Fig. 3. Microdevice for fish freshness determination. (A) Expanded view. (B) Top view showing the layout of the flow channel network and sensor. The figure in the bottom right shows the structure under the PDMS substrate. Reprinted with permission from Itoh et al. (2012).

9. Microfluidic applications highlights

In most microfluidic biosensing applications, the analyte of interest needs to diffuse to the biorecognition-sensing element, which is immobilized on a surface. Flow cell geometry therefore has a strong impact on the performance of affinity-based biosensors. Lynn et al. (2013) showed that the reduction of the flow cell height can have drastic effects on the performance of an SPR-based biosensor. The LOD for the detection of ssDNA decreased by a factor of 4 when the cell height was reduced from 47 µm to 7 µm. On the other hand, Cohen et al. (2015) overcame the adsorption kinetics reaction rate-limiting mechanism, which is diffusion-controlled in standard immunoassays, by introducing the microsphere-based assay into a simple microfluidic device which performs mixing of the sample with turbulent flow profiles in the reaction regions.

Most optical-based biosensors rely on conventional laboratory instrumentation for detection, losing the main advantages of portability and simplicity. However, some groups have worked on the implementation of optical sensing elements directly on the microfluidic platform. Duval et al. (2012) developed a nanophotonic biosensor, the bimodal waveguide (BiMW) interferometer, for direct on-chip detection. The authors integrated bimodal waveguide interferometers with sub-micronic grating couplers for efficient light in-coupling on a SU-8 microfluidic chip (Fig. 4).

Other efforts have focused on developing portable readout instrumentation. For example, Donolato et al. (2015) presented a high-performance low-cost readout of a homogeneous assay using a Blu-ray optical pickup unit (Fig. 5). The assay relies on optical measurements of the dynamics of magnetic nanobeads in an oscillating magnetic field applied along the light propagation direction. The authors demonstrated that beads bound to coils of DNA show different dynamics than freely rotating magnetic nanobeads. Using this system, the authors have achieved a LOD of 10 pM and a dynamic range of about two orders of magnitude, which is comparable to the performance obtained using costly and bulky laboratory equipment. Novo et al. (2014) presented a point-of-care prototype system by integrating capillary microfluidics with a microfabricated photodiode array and electronic instrumentation into a hand-held unit (Fig. 6). The platform integrated fluid flow control and the photodiode signals were acquired, displayed and processed by a simple graphical user interface using a computer. The prototype performed integrated chemiluminescence ELISA detection in about 15 min with a limit-of-detection of 2 nM for a model chemiluminescence assay, a performance comparable to traditional bench-top instrumentation. Personal intelligent devices, such as smartphone cameras, can also be used to enhance portability and simplicity. Chun et al. (2014) presented a paper-based glucose biosensing system utilizing a smartphone as a signal reader for the colorimetric assay. Li et al. (2014a) utilized a smartphone to control elastomeric on-chip valves. In Comina et al. (2015) the authors compared several commercially available smartphones for implementation in quantitative glucose metering. The LOC device integrates finger pumps, unidirectional valves, calibration references and focusing optics.

Microfluidic devices can also be used to generate sensing elements in-situ. Seefeld et al. (2012) developed the on-chip, cell-free synthesis of a protein microarray from a DNA microarray, which can diffuse from the generator element directly to the detector element of the chip and be used immediately for SPR protein biosensing (Fig. 7). SadAbadi et al. (2013) advantageously used the reducing properties of the cross-linking agent present in PDMS to synthesize AuNPs in a PDMS microfluidic chip in-situ prior to SPR sensing. Synthesis of nanoparticles in the microfluidic environment resulted in a marked improvement of the size distribution with only 8% variation, compared with the macro-environment that yielded about 67% variation in size.

Microfluidic platforms are increasingly being used for monitoring cell activity and provide an ideal platform for the implementation of whole-cell biosensors. Roda et al. (2013) took advantage of the properties of magnetotactic bacteria, using microfluidics to move the cells between the incubation and detection

Table 3
Summary of recent advances in fluorescence-based biosensors in microfluidic applications.

Analyte	Biological recognition element	LOD and/or linear range	Microfluidic chip features	Reference
Cocaine	FITC-labeled aptamer immobilized on PDMS	0.2 μM	Fluorescence measurements on a PDMS surface (no fluidics)	Zhou et al. (2012)
H5N1 antigen	Anti-H5N1 antibodies conjugated to polydiacetylene vesicles (PDAVs) onto the surface of polystyrene (PS) microspheres	30 ng mL^{-1} (absorbance) or 1 ng mL^{-1} (laser scanning confocal microscopy)	Only stability tested in a PDMS microchannel	Dong et al. (2013)
$CdCl_2$	Genetically modified sensor cells based on the human keratinocyte cell line HaCaT transfected with a HSP72-GFP reporter plasmid	7 μM	Used commercially available "μSlides" (Ibidi, Germany) to monitor cell cytotoxicity fluorescence and impedimetric measurements	Hofmann et al. (2013)
Genes expressed by pathogenic strains of *Escherichia coli* O157:H7	DNA capture probes	n.a.	Uses optical tweezers not applied yet to microfluidics	Manesse et al. (2013)
Thrombin, cytochrome C, lysozyme	DNA aptamers, targeting thrombin, cytochrome C, lysozyme	n.a.	FRET using graphene oxide includes capillary electrophoresis separation	Lin (2014)
Cardiac troponin I (cTnI)	Monoclonal anti-cTnI capture antibodies	24 pg mL^{-1}	PMMA and double-sided adhesive tape (3 M™ Adhesive Transfer Tape 9626) device on-chip lenses machined with CO_2 laser	Mohammed and Desmulliez (2014)
Arsenic	*Escherichia coli* bioreporter cells encapsulated in agarose	10–100 μg As L^{-1}	PDMS device with complete optical illumination/collection/detection system powered by a 12 V power supply	Truffer et al. (2014)
E. coli	Aptamer-conjugated fluorescent nanoparticles (FluoSpheres®)	Single cells	PDMS	Chung et al. (2015)
Galactose	Monolith bound galactose oxidase	n.a.	Thiol-ene monolith	Lafleur et al. (2015)
Calf thymus DNA	$Ru(bpy)_2(dppx)^{2+}$	1.0 pg	PDMS device for droplet microfluidics	Xiang et al. 2012a
dsDNA Hg(II)	Syber Greenhairpin-Hg	4.5 nM (HIV) 12 nM (Hg)	PDMS device for droplet microfluidics	Chen et al. (2015a)
ssDNA	FAM-ssDNA ROX-ssDNA	9.46×10^{-8} M 9.67×10^{-8} M	Droplet-based biosensor using graphene oxide	Xiang et al. (2012b)
Hg^{2+} Ag^{+} aminoglycoside antibiotics residues in food (NEO)	ssDNA functionalized graphene oxide	121 nM (Hg^{2+}) 47 nM (Ag^{+}) 153 nM (NEO)	Paper microfluidics	Zhang et al. (2015)
Salmonella cells	Anti-salmonella polyclonal antibodies covalently immobilized on the quantum dots	10^3 CFU mL^{-1}	Uses superparamagnetic particles to separate and concentrate the sample and developed a portable fluorometer.	Kim et al. (2015)
Tumor necrosis factor (TNF)-α anti-TNF-α antibody	Anti-TNF-α microsphere-based sensors	0.02 ng mL^{-1} (TNF-α) 100 ng mL^{-1} (anti-TNF-α)	PDMS device featuring both laminar and turbulent flow profiles in distinct regions of the device	Cohen et al. (2015)
Measurement of fluid shear stress (FSS)	Whole cell	2 dynes cm^{-2}	Inertial microfluidic device environment with typical flow conditions to study the impact of FSS.	Varma and Voldman (2015)
Aptamer-conjugated target analytes (oral cancer biomarker)	Aptamer-functionalized microtubules	n.a. (detected 10 fM)	Transport by electrophoresis and sieving on a nanoporous hydrogel	Kim and Kim 2014
HIV-p24 antigen	Monoclonal anti-p24 antibodies -coated polystyrene microbeads	2–130 pg mL^{-1}.	Features smartphone controlled elastomeric on-chip valves and a compact pneumatic system	Li et al. (2014a)
Hyper-methylated DNA (hm-DNA)	Methyl-binding domain capture proteins	capture and elution of ≤ 1 ng ml^{-1} hm-DNA	Features a pillar array for microfluidic solid phase extraction	De et al. (2014)
Adenosine cocaine	Aptamer functionalized microbeads	0.1 pM (adenosine) 0.5 pM (cocaine)	Combines a microfluidic bead-based array chip with nanoparticle amplification and quantum dots labels	Zhang et al. (2014)
Prostate-specific antigen	Antibody-functionlized QD-encoded microbeads	1 ng mL^{-1}	Microfluidic device that combines suspension and the planar microarray format	Han et al. (2015)

Table 3 (*continued*)

Analyte	Biological recognition element	LOD and/or linear range	Microfluidic chip features	Reference
Cholera toxin in stool samples	Superparamagnetic beads immobilized antibodies	9.0 ng mL^{-1}	Mixing, capture and detection on-chip as well as electrochemical detection	Bunyakul et al. (2014)
Bisulfide	Functionalized nanoparticle–glutathione-fluorescein isothiocyanate probe	2 μM/5 μM to 50 μM	Droplet-based microfluidic chip/micro-dialysis system	Zhu et al. (2014)
DNA, streptavidin	ssDNA-Cy3 optical molecular beacon probes on Au surface	1 pM (60 amol) (streptavidin)	Simple line-shape microfluidic channel	Wang et al. (2014a)
Cancer cells	Aptamer/graphene oxide (GO) complex	25 cells mL^{-1}/2.5×10^1–2.5×10^4 cells mL^{-1}	Quantitative assay of 7 different cell samples at the same time by utilizing a parallel-scale homogenous detection	Cao et al. (2012)
DNA	Nucleic acid modified magnetic beads and $Ru(bpy)_3^{2+}$ doped silica nanoparticles	1 pmol	PMMA device enclosing an absorbent pad; the device combined elements of lateral flow assays and microfluidic technology	Jin et al. (2012)
Glucose alcohol	Glucose oxidase and alcohol oxidase conjugated CdSe/ZnS QDs and entrapped within a hydrogel	50 μM (glucose) 70 μM (alcohol)	The biosensor consists of three components (quantum dot–enzyme conjugates, hydrogel microstructures, and a set of microchannels) that were hierarchically integrated into a microfluidic device	Jang et al. (2012)
Mercury	BSA coated AuNC	0.6–60 μg L^{-1}	PDMS mixing device	Lafleur et al. (2012)
DNA	AgNP-bound DNA hairpin probes immobilized on glass	500 pM	Simple flow cell nanoplasmonic PDMS device	Peng et al. (2012)
Bisphenol A (BPA)	Fluorescence-labeled anti-BPA monoclonal antibodies	0.06 μg L^{-1}/0.5–100 μg L^{-1}	Tapered fiber optic sensor embedded in PMMA microfluidic device	Long et al. (2014)
FAM labeled DNA	Probe DNA immobilized on paramagnetic beads	42.9 pM	Glass chip and magnetic button for paramagnetic beads capture with detection in real saliva samples; short analysis time (15 min)	Wang et al. (2013c)

Abbreviations: Limit of detection (LOD), polydimethylsiloxane (PDMS), polymethylmethacylate (PMMA), cyclic olefin copolymer (COC), single-stranded DNA (ssDNA), double-stranded DNA (dsDNA), gold nanoparticle (AuNP), gold nanorods (AuNR), green fluorescent protein (GFP), bovine serum albumin (BSA), gold nanoclusters (AuNC), silver Nanoparticles (AgNP), quantum dots (QD), fluorescein (FAM).

Table 4
Summary of recent advances in label-free biosensors and other non-fluorescence-based optical biosensors in microfluidic applications.

Analyte	Biological recognition element	LOD and/or linear range	Microfluidic chip features	Reference
Evanescent-wave sensors				
Rabbit anti-goat IgG antibody	Non-specific protein adsorption	1×10^{-5} RIU or 200 ng mL^{-1} protein	Pyrex glass /oxidized silicon optical elements (grating, waveguides) combined with microfluidic channels (simple flow chamber) cut-out in double-sided adhesive tape with a glass lid	Grego et al. (2012)
Listeria monocytogenes	Anti-listeria. monocytogenes immobilized on TiO_2 film	n.a. (detected concentrations as low as 10^6 CFU mL^{-1})	Birefringent waveguide biosensor	Sim et al. (2012)
Optical resonators				
Prostate specific antigen (PSA)	Anti-PSA antibody	n.a.	Refractive index sensing using microring resonators combined with commercial chips (Genalyte Inc., CA, USA)	Marty et al. (2012)
Streptavidin	Phospholipid ink (biotin)	n.a.	PMMA device featuring photonic whispering gallery mode resonators and on-chip micro lasers	Bog et al. (2013)
β-blockers	Endogenous β_2-adrenergic receptor (β_2-AR) ligands in A431 cells	n.a	PDMS device featuring a label-free resonant waveguide grating (RWG) biosensor providing a real-time dynamic mass redistribution (DMR) signature	Ferrie et al. (2013)
Streptavidin *E. coli* bacteria	Unspecific serospecific polyclonal antibody probes	1 pg mm^{-2} (streptavidin)10^6 CFU mL^{-1} (*E. coli*)	Microfluidic sample delivery channels are fabricated monolithically on the chip the chip features a silicon photonic wire waveguide folded into a spiral ring resonator	Janz et al. (2013)
Streptavidin	Anti-streptavidin	3×10^{-4} RIU (intrinsic LOD determined using NaCl)	Silicon sensing device integrated with PDMS microfluidics and refractive index sensing using phase-shifted Bragg gratings in a slot wave-guide	Wang et al. (2013a)
Mouse IgG	Biotinylated anti-mouse antibody	n.a.	SU-8 polymer dual ring resonator	Salleh et al. (2013)
Surface Plasmon Resonance (SPR, LSPR)				
Type A red blood cells	Antibodies against type A red blood cells	2.3×10^{-6} RIU (bulk sensing)	Long-range surface plasmon-polariton (LRSPP) channels and waveguides etched in CYTOP™	Krupin et al. (2013)
Soluble cell-surface glycoprotein sCD44	Anti CD44 antibody	10.53 pM	Device fabricated in thermoplastics by hot embossin; features monolithic integration of blazed nanogratings and pneumatic valves	Malic et al. (2013)
Six cytokines in a complex serum matrix	Antibody-functionalized AuNR	11.43 pg mL^{-1} (TNF-α), 6.46 pg mL^{-1} (IFN-γ), 20.56 pg mL^{-1} (IL-2), 4.60 pg mL^{-1} (IL-4), 11.29 pg mL^{-1}(IL-6), and 10.97 pg mL^{-1} (IL-10)	Multiplex assay on a glass-PDMS device featuring a AuNR array	Chen et al. (2015b)
Bovine growth hormone (BGH)	Anti-BGH coated gold nanoparticles	3.7 ng mL^{-1} (185 pM)	AuNPs synthesized in-situ in PDMS device prior to SPR sensing	SadAbadi et al. (2013)
20-mer oligomers of ssDNA	Biotinylated oligonucleotides	5 pM	Demonstrates that the reduction of the flow cell height can have drastic effects on the performance of an SPR-based biosensor	Lynn et al. (2013)
Ovarian cancer marker r-PAX8	Ovarian cancer marker antibodies	5 nM LOD/0.25–9.0 μg mL^{-1}	Nanohole array-based biosensors integrated with a microfluidic concentration gradient generator	Escobedo et al. (2013)
RS-melagatran	Human α-thrombin immobilized onto AuNR	0.9 nM	AuNRs were self-assembled onto the surface of the inner wall of the glass microfluidic chip to serve as LSPR transducers	Guo et al. (2012)

Table 4 (*continued*)

Analyte	Biological recognition element	LOD and/or linear range	Microfluidic chip features	Reference
Anti-GFP and antiluciferase	GFP and luciferase	n.a.	Protein microarray generated directly on-chip for SPR sensing	Seefeld et al. (2012)
Interferometry				
Human thyroid stimulating hormone (hTSH)	hTSH antigen	3.3×10^{-7} RIU, picomolar detection of hTSH	PDMS device, integrated waveguides (Si_3N_4/SiO_2), grating couplers and electronic data processing	Duval et al. (2012)
Circulating tumor cells (pancreatic cancer cells)	Anti-EpCAM antibody	$<$ 1000–100,000 cells mL^{-1}	PMMA device with simple mixers and nanoporous anodic aluminum oxide sensing surface for label-free reflectometric interference spectroscopy	Kumeria et al. (2012)
Glucose Galactose Ethanol	Glucose oxidase Galactose oxidase Alcohol oxidase	n.a. sensitivity: 0.51 pm mol^{-1} (glucose) 2.45 pm mol^{-1} (galactose) 0.63 pm mol^{-1} (ethanol)	SU-8 device featuring Au electrodes – readout obtained by scanning the electrical double layer optically	Lee and Saraf (2014)
Scattering				
Cryptosporidium parvum	Anti-C. parvum conjugated polystyrene beads	single oocyst/ 5 orders of magnitude linear range	PDMS/Y-shape mixer, integrated waveguides	Angus et al. (2012)
Escherichia coli DNA coils	Oligonucleotide coated magnetic nanobeads	10 pM of Escherichia coli DNA coils/ca. 2 orders of magnitude linear range	PMMA/centrifugal microfluidics integrated with Blue-ray optical pickup	Donolato et al. (2015)
Viral RNA	Nucleotide probe – coated magnetic beads	25 fg	Integrated with optical fibers and micro-stirring	Lin et al. (2015)
Colorimetric, absorbance				
Glucose	Glucose oxidase	23.8 μmol L^{-1}/0.1–2.5 mmol L^{-1}	Optofluidic sensor with channels machined directly in the surface of a LED	Cocovi-Solberg et al. (2012)
Propofol	Molecularly imprinted polymers	0.0792–7.918 μg mL^{-1}	Molecularly imprinted polymer, COC chip substrate	Hong et al. (2012)
Casein	Anti-casein antibody	100 ng mL^{-1} to 1 mg mL	Simple PDMS/glass microfluidic device	Zhang et al. (2013)
Glucose	Glucose oxidase, horseradish peroxidase	0.7 mM (buffer standards) and 0.3 mM (human serum)	Paper microfluidic device with smartphone readout	Chun et al. (2014)
β-hydroxybutyrate (βHBA)	βHBA dehydrogenase	0.05 mM	PDMS chip featuring mixing, incubation and reaction chambers	Weng et al. (2015)
Cadmium, chromium, lead	AuNP immobilized antibodies	0.57–60.06 ppb (Cd) 0.03–0.97 ppb (Cr) 0.04–5.28 ppb (Pb)	PDMS chip featuring a PMMA packed solid phase	Date et al. (2012)
Glucose	Glucose oxidase, horseradish peroxidase	n. a.	Quantitative glucose metering with integrated finger pumps, unidirectional valves, calibration references and focusing optics using a smartphone	Comina et al. (2015)
Chemical luminescence				
Anti-rabbit IgG	Rabbit IgG antibody	2 nM	PDMS device with integrated optical detection setup and chemiluminescence detection	Novo et al. (2014)
DNA amplicons	DNA probe	6.3×10^{-2}–1.94×10^{4} pmol L^{-1}	Paper based microfluidic device with chemiluminescence detection	Liu and Zhang 2015

Nalidixic acid (NA) Hydroquinone (HQ)	Whole cells	5 μg mL^{-1} – (NA) 2 μg mL^{-1} – (HQ)	Bioluminescence whole cell sensor array biochip featuring an integrated temperature control and a 16-member sensor array	Tsai et al. (2015)
ssDNA	DNA capture probe covalently bound to AgNPs on the surface of $CaCO_3$/CMC hybrid microspheres	8.5×10^{-18} M/4.0×10^{-17}–5.0×10^{-11} M	Graphene-modified porous Au-paper for electrochemiluminescence	Li et al. (2014b)
Dimethyl sulfoxide and a bile acid (taurochenodeoxycholic acid)	Magnetospirillum gryphiswaldense		Multilayered black and transparent PDMS chip; bioluminescent magnetic bacteria are moved by microfluidics and trapped and concentrated in detection chambers by an array of neodymium–iron–boron magnets	Roda et al. (2013)
Parvovirus B19	Oligonucleotide array	80 pmol L^{-1} (B19 genotype oligonucleotides) 650 pmol L^{-1} (amplified product of B19 genotype 1)	The portable device consists of a reaction chip, comprising a glass slide arrayed with three B19 genotype-specific probes, and coupled with a PDMS microfluidic layer for multiplex detection	Mirasoli et al. (2012)

*Abbreviations used: Abbreviations: Limit of detection (LOD), polydimethylsiloxane (PDMS), polymethylmethacrylate (PMMA), cyclic olefin copolymer (COC), single-stranded DNA (ssDNA), double-stranded DNA (dsDNA), gold nanoparticle (AuNP), Refractive index unit (RIU), gold nanorods (AuNR), green fluorescent protein (GFP).

areas of the chip where they were trapped by an array of neodymium–iron–boron magnets. However, the fluid flows generated within microfluidic systems can generate fluid shear stress (FSS). In microfluidic systems designed for cell-based studies, this FSS may adversely affect cell health. Varma and Voldman (2015) developed and tested genetically encoded cell sensors that fluoresce in a quantitative fashion upon FSS pathway activation. These cell sensors could allow microfluidic device designers and end-user to evaluate the impact of FSS upon their assay of interest.

Ultimately, no transduction system is perfect and microfluidic devices offer the unique possibility to implement more than one sensor on a chip. Bunyakul et al. (2014) demonstrated that orthogonal detection approaches, such as the fluorescent and electrochemical systems, can assist in the identification of matrix effects of the transduction system itself.

10. Microfluidic biosensors based on micromechanical transduction

Micromechanical transducers all work on the principle of translating a mechanical exertion on a material, in the form of force, displacement or mass change, into a detectable signal, either directly or indirectly (Arlett et al., 2011; Tamayo et al., 2013). This can be achieved through a number of different methods: surface stress based sensors (Sang et al., 2014), such as microcantilevers (Porwal et al., 2002) and membrane biosensors (Sang and Witte, 2010), where the binding of molecules to the material surface results in a deflection of the material through electrostatic attraction or repulsion between the bound molecules; resonance sensors (Bunde et al., 1998), such as quartz crystal microbalances (QCM) (O'Sullivan and Guilbault, 1999) and acoustic sensors (Voinova, 2009), where the binding of a cell or molecule changes the resonance frequency of the sensor material; and conductive sensors (Ramanathan et al., 2005), such as nanowire sensors (Patolsky et al., 2007; Zhang and Ning, 2012) where the binding of a cell or molecule changes the capacitance of the sensor material. A summary of recent studies utilizing micromechanical sensors of the above-mentioned types in microfluidic applications can be found in Table 5.

11. Cantilevers

In microfluidics, and by extension potential lab-on-a-chip applications, the use of cantilevers is still the dominating transduction method in the micromechanical field. A common realization is the incorporation of functionalized cantilevers directly in a microfluidic channel where they are exposed to the flow of a sample solution, allowing the target analyte to come into contact with sensing material present on the cantilever surface. Depending on the composition of the cantilever this can lead to deflection of the material, but cantilevers are also intrinsically suited to work as resonance sensors, replacing QCMs in microfluidic applications. Regardless of the transduction method, cantilevers are generally used for direct detection of biological substances through binding of a sensing element to the sensor surface. Antibodies are by far the most commonly employed biorecognition elements as they provide both a strong and specific binding to the target analyte. This yields LODs in the nanomolar range (Bache et al., 2013; Yen et al., 2013) for proteins, but also routinely in the picomolar range (Park et al., 2012) and even, in some cases, into the attomolar range (Yin et al., 2013). Also commonly used are DNA capture probes, allowing, e.g., detection of harmful pathogens, such as HIV in blood at a nanomolar range (Alodhayb et al., 2013), and aptamers for detection of proteins (Bosco et al., 2013).

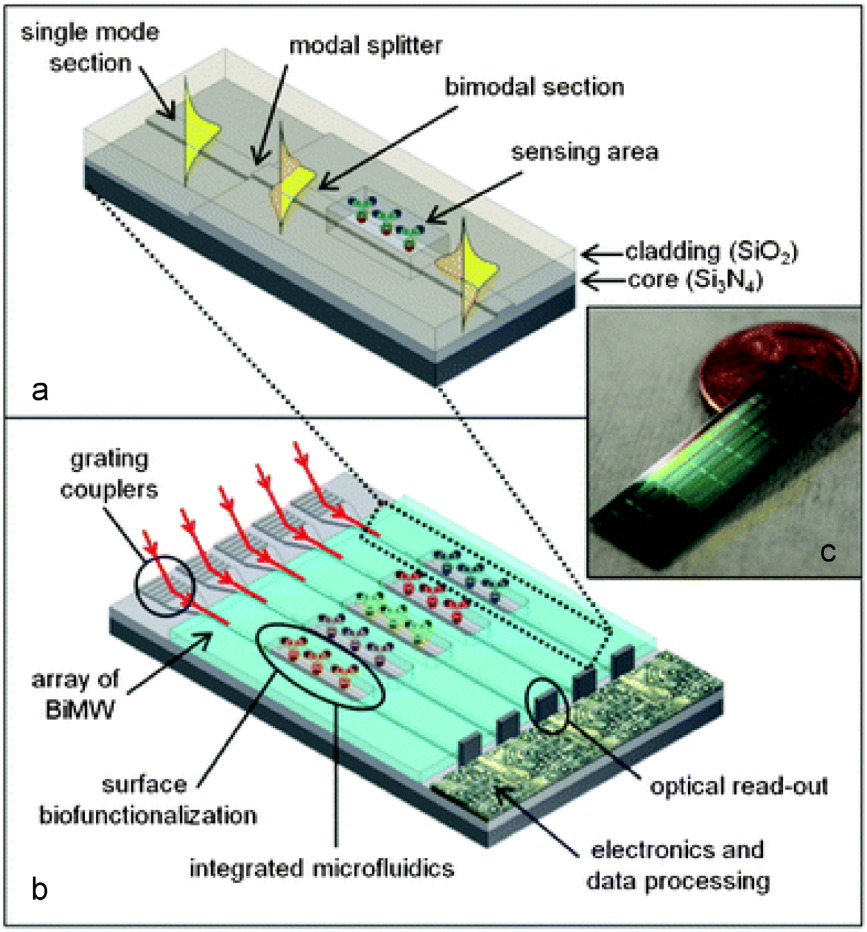

Fig. 4. (a)Scheme of the bimodal waveguide (BiMW) interferometer highlighting the distribution of the electromagnetic field in the single mode and the bimodal sections. (b) Scheme of the envisioned LOC platform based on BiMW sensors. (c) Photograph of a chip of 30 × 10 mm^2 containing 16 BiMW interferometers. Reprinted with permission from Duval et al. (2012).

On the less conventional side, cantilevers have also been used in determining antibiotic resistance in bacteria (Longo et al., 2013), where the death of an immobilized cell leads to a shift in surface deflection, as well as identification of double stranded DNA (Xu et al., 2014), where DNA is labeled, immobilized and subsequently digested at specific cleavage sites, resulting in a characteristic change in resonance. With multiple inlets for sample, enzyme, and buffer, this can be seen as a simple lab-on-a-chip device (Fig. 8).

Independent of sensing element and transduction method, cantilevers so far see a limitation in their usability for lab-on-a-chip applications stemming from the lack of continuous detection solutions. As is the case for many other biosensors, the immobilized sensing element must be regenerated by the removal of bound analyte, therefore requiring washing steps between each analysis, making cantilevers ill-suited for monitoring purposes in applications such as cell cultivation.

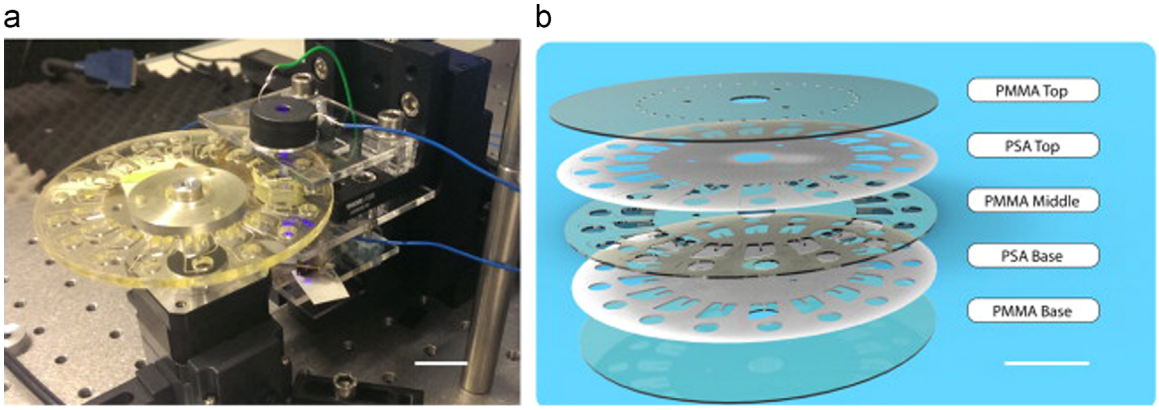

Fig. 5. Picture of a sensing platform incorporating a Sanyo Blu-ray optical pickup unit as a core element. (b) Schematic of the different PMMA and PSA layers forming the structure of the microfluidic disk. The scale bars indicate a length of 2 cm. Reprinted with permission from Donolato et al. (2015).

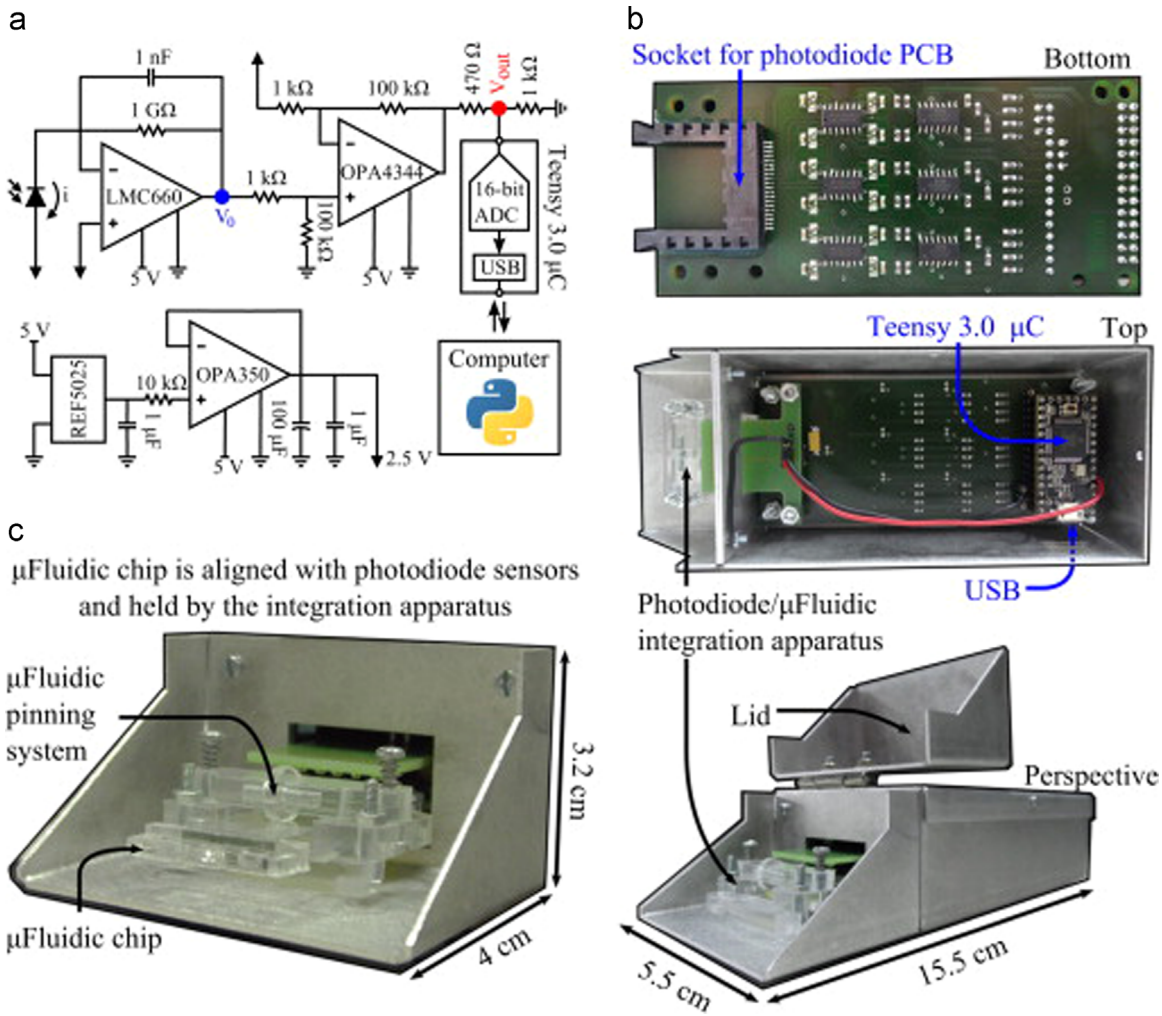

Fig. 6. Point of care prototype device details. (A) Photodiode amplification circuit schematics, (B) a hand-held prototype box: (top) bottom view of the amplifier circuit board highlighting the socket where the printed circuit board is inserted; (middle) top view of the prototype box containing the amplifier circuit and the Teensy 3.0 microcontroller; (bottom) perspective view of the closed aluminum prototype box and (C) magnified perspective view of the microfluidics integration apparatus: the photodiode PCB and machined PMMA ensemble align and fix the microfluidic device to the photodiodes. Reprinted with permission from Novo et al. (2014).

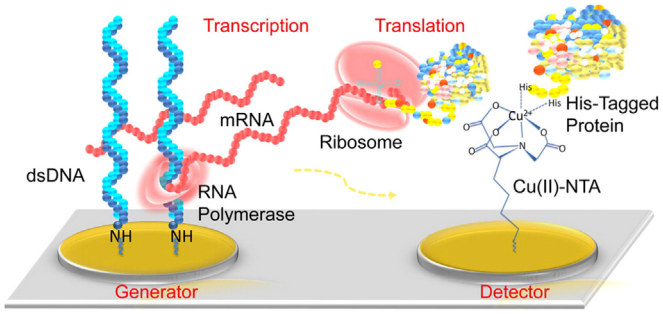

Fig. 7. Schematic diagram of the on-chip synthesis of protein microarray from DNA microarray via surface in vitro transcription–translation. On the generator elements, the encoding dsDNA was covalently attached to the gold surface and mRNA was transcribed with T7 RNA polymerase. Translated His-tagged protein diffused to the adjacent detector elements and was captured by Cu(II)-NTA surface. Reprinted with permission from Seefeld et al. (2012).

12. Acoustic sensors

A variation on resonance sensing, acoustic sensors offer a robust alternative to the resonance cantilevers. They are often divided into surface acoustic wave (SAW) and bulk acoustic wave (BAW) sensors with the difference being how the acoustic waves propagate through the sensor material. In both cases the sensor consists of a transmitting electrode and a receiving electrode, connected by a resonating material. In the case of microfluidic biosensors, only the resonator is included in the channel and it is on this surface that the sensing element can be attached. While not as common as the cantilever sensors, acoustic sensors have nonetheless recently been shown to provide highly sensitive detection of bacteriophages (Matatagui et al., 2013) and Jurkat cells (Hao et al., 2013), using SAW, and pesticides (Chen et al., 2013), using BAW, with antibodies as sensing elements. Demonstrating the versatility of the acoustic sensors, (Gammoudi et al., 2014) have also shown the detection of heavy metals in aqueous media utilizing immobilized *E. coli*. The metabolic changes induced by the heavy metals in the bacteria result in a detectable shift in resonance, with a LOD of < 1 pM for cadmium and mercury.

The non-invasive nature of acoustic sensors enables detection in potential lab-on-a-chip applications without disturbing the microfluidic channel geometry, providing a robust and easily integrateable sensor. The direct mechanism of detection does, however, limit its use in continuous detection.

13. Conductive sensors

While it is the conductivity of the sample solution that is being

Table 5
Summary of recent studies utilizing micromechanical biosensing in microfluidic applications.

Analyte or detected mechanism	Biological recognition element	Limit of detection (LOD)	Microfluidic chip features	Reference
Deflection				
HIV-DNA	ssDNA	0.2 nM	Flow cell with 8 silicon cantilevers in a circle formation	Alodhayb et al. (2013)
PDGF	Aptamer	10 nM	CD-like PMMA flow cell with cantilevers; DVD-ROM optical unit for detection	Bosco et al. (2013)
Antibiotic resistance	*E. coli, S. aureus*	N/A	Flow cell with single cantilever	Longo et al. (2013)
Troponin I	antibody	1 pg mL^{-1} (~42 aM[a])	PDMS flow cell microcantilever sensor based on contact angle analysis	Yin et al. (2013)
suPAR	antibody	5 nM	CD-like PMMA/glass flow cell with cantilevers; DVD-ROM optical unit for detection	Bache et al. (2013)
CRP	antibody	1 μg mL^{-1} (~8 nM[a])	PDMS flow cell with single free-standing piezo-resistive microcantilever	Yen et al. (2013)
Resonance				
DNA-cleaving	streptavidin, DNA-probe	8.8 pg Hz^{-1}	PDMS flow cell with silicon cantilevers	Xu et al. (2014)
Insulin	antibody	0.4 ng mL^{-1} (~70 pM[a])	PDMS flow cell with microcantilever resonating at air–liquid interface	Park et al. (2012)
M13 bacteriophage	Antibody	$5*10^7$ pfu mL^{-1}	PDMS flow cell with cross channel Love-Wave sensor	Matatagui et al. 2013
Heavy metals (cadmium, mercury)	*E. coli*	< 1 pM	PDMS flow cell with Love-Wave sensor	Gammoudi et al. (2014)
Pesticide (carbaryl)	Antibody	3.2 ppb (~16 pM[a])	Flow cell with FBAR biosensor	Chen et al. (2013)
Jurkat cells	Antibody	10^3 cells mL^{-1}	PMMA flow cells with SH-SAW sensors	Hao et al. (2013)
Conductivity				
Myoglobin, troponin I, CK-MB, BNP	Antibody	50 fg/ml (BNP) (~14 fM[a])	PMMA flow cell with PANI nanowire sensor	Lee et al. (2012)
ssDNA-RecA-dATP Interaction	ssDNA	250 RecA molecules	PDMS flow cell with silicon nanowire sensor	Chiesa et al. (2012)
Thyrotropin	Antibody	0.5 mIU L^{-1} (89 nM[a,b])	PDMS flow cells with silicon nanowire sensor arrays	Hemmilä et al. (2014)
DNA hybridization	PNA	N/A	PDMS flow cells with silicon nanowire sensor arrays	De et al. (2013)
Streptavidin	Biotin	0.6 pM	PDMS/SU-8 flow cell with silicon nanoribbon sensors	Björk et al. (2014)

Abbreviations used: single stranded DNA (ssDNA), platelet-derived growth factor (PDGF), polymethylmethacrylate (PMMA), polydimethylsiloxane (PDMS), soluble urokinase-type plasminogen activator receptor (suPAR), C-reactive protein (CRP), thin-film bulk acoustic resonator (FBAR), shear horizontal-surface acoustic wave (SH-SAW), creatine kinase type MB (CK-MB), brain natriuretic peptide (BNP), polyaniline (PANI).

[a] Conversion by author.
[b] 0.2 ml U/mg (Mariotti, 2011).

monitored in conductometry, micromechanical conductive sensors rely upon changes in the conductivity of the sensor material itself.

Conductive nanowires are generally used for direct detection of analytes through immobilized affinity recognition elements. The binding of an analyte to such a sensing element changes the conductivity of the nanowire material, resulting in a measurable decrease in current. Recent studies using antibodies as sensing elements have demonstrated LODs down to the femtomolar range for certain substances such as pesticides (Chen et al., 2013), small peptides (Lee et al., 2012), and hormones (Hemmilä et al., 2014). Conductive nanowires have also been used in more qualitative sensing where interactions between a DNA repair protein (RecA) and single stranded DNA can be detected with as few as 250 RecA molecules (Chiesa et al., 2012). In another study, peptide nucleic acid (PNA) has been used to follow DNA:PNA hybridization in terms of kinetics, finding the related affinity constants (De et al., 2013). A variation on the nanowire concept, nanoribbons have recently been investigated for biosensing using biotin as sensing element for streptavidin, providing a first proof of concept (Björk et al., 2014).

The large variety of applications for conductive nanowire biosensors in recent publications suggests that it is an attractive method, with great potential, for research in diverse areas. So far, the limitation of the method seems to be the lack of possibilities for continuous detection, a drawback that is ever present for the micromechanical sensors at large.

14. Miscellaneous

14.1. Thermometric

Thermometric or calorimetric sensors typically measure heat (change in enthalpy or change in temperature) as a result of a biochemical reaction or interaction, and transduce this change into an electrical signal. Lee and co-authors provide a general overview over microchip-based calorimeter designs (Lee et al., 2012). Miniaturized calorimeters are excellent tools for measuring binding affinities, which makes them highly relevant for biosensing applications. The miniaturization also improves the time constants associated with the measurements such that these devices can potentially be used for high throughput screening. The authors describe a variety of realizations of chip calorimeters, different designs and different operation modes. Application examples in biosensing are also given, as well as some discussion on how to fluidically address the sensors. Here, the thermal properties of the chosen materials are especially important since the relatively large mass surrounding the channels can lead to an effective “sinking” of heat, which has implications on the performance of the sensor.

Yakovleva et al. have recently published an article describing

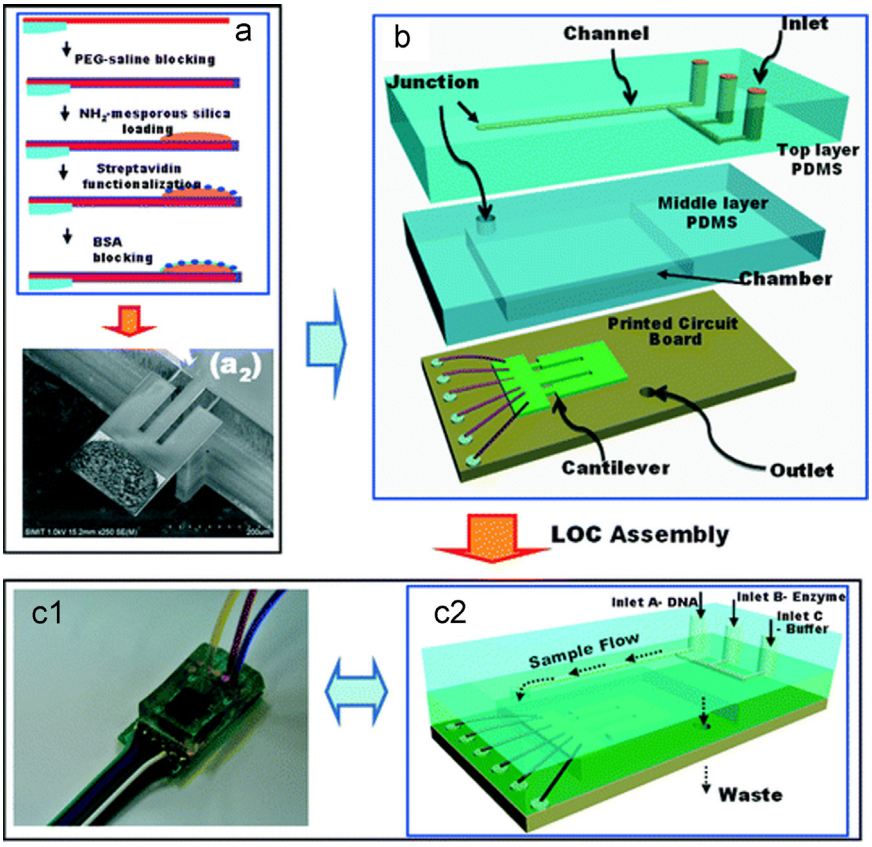

Fig. 8. The construction of the resonant cantilever embedded LOC for the online analysis of a acoustic sensors. Reprinted with permission from Xu et al. (2014).

enzyme thermistors, which, according to the authors, have the potential to become almost universal biosensors (Yakovleva et al., 2013). In these devices, typically an enzyme reactor is coupled to a thermistor, but other types of biorecognition elements can also be used, such as whole cells, organelles or even tissue. These sensors are often used in flow analysis settings, but the thermistor does not need to be in fluidic contact with the enzyme reactor or the effluent from this reactor, thus preventing fouling of the sensor surface. While a label-free technique, measurement of a temperature is not very specific. Some selectivity is then provided by, e.g., the choice of enzyme. The authors describe the versatility of enzyme thermistors for biosensing applications as well as different designs. Those to be incorporated in microfluidic systems are discussed, but the emphasis is mainly on the sensor components and not so much on the fluidic parts.

Another microfluidic biosensor chip using a calorimetric transducer was published by (Davaji and Lee, 2014). Here, the fluidic transport is facilitated by a paper strip. In paper-based microfluidics, the capillary action of the paper fiber network is utilized to transport chemicals without the need for external pumps or an external electric field. In the authors' work, a paper strip is impregnated with an enzyme at a specific location and sample is moved over the strip by capillary action. When the analyte arrives at the site of the enzymes the reaction starts and the enthalpy change is measured (see Fig. 9). Feasibility of the design was tested for glucose detection using glucose oxidase as the immobilized enzyme.

In a final example, Trantum et al. utilized temperature changes in a very different way to facilitate biosensing (Trantum et al., 2013). They used antibody-covered microbeads inside small droplets that were deposited onto a surface. Directed by the thermal properties of the surface material and the cooling of the droplet surface due to evaporation, so called Marangoni flows were induced inside the droplets, transporting the beads closer together and towards the center of the droplet. If the antigen was present, immunoagglutination would happen, resulting in a visually detectable spot. No antigen present would correspond to no spot, while increasing concentrations of antigen would give increasing spot sizes. An LOD of about 100 fM for a bacteriophage detection was reported. While this represents the simplest microfluidic realization possible, and does not really include a thermal transducer, it is a good example of the fantastic variety of biosensors researchers have developed and continue to devise.

15. Magnetic sensors

In the field of magnetic transduction there are two major types of sensors that are both used to detect the presence of magnetic microbeads: magnetoresistive sensors and Hall-type sensors (Llandro et al., 2010).

Magnetoresistive sensors work by a magnetic field changing the resistance of a material, in this case the sensor. A magnetic field is applied over the sensor and any magnetic bead in close proximity. This induces a magnetic dipole in the bead, the magnetic field of which changes the resistance of the sensor material. The change in voltage this leads to can then be detected (Wang and Li, 2008).

In the case of Hall sensors a current is applied through a conductor material in the presence of an external magnetic field. This pushes the charge carriers to one side of the conductor, resulting in a transverse electrical field with a potential known as the Hall voltage. When a paramagnetic bead enters the magnetic field an internal magnetic field is formed. This field is parallel to the external field. When the bead comes in close proximity to the conductor a change in the Hall voltage can be detected due to the

interaction of the magnetic fields (Besse et al., 2002). A summary of recent studies utilizing magnetic sensors of the above-mentioned types in microfluidic applications can be found in Table 6.

16. Magnetoresistive sensors

Similar to micromechanical conductive biosensors, magnetoresistive biosensors transduce the biological sensing event by measuring a change in resistance of the sensor material. The major difference between the two methods being that the magnetoresistive sensor detects the analyte indirectly through labels consisting of one or several magnetic nanobeads. Recent studies have successfully utilized both antibodies and DNA-probes as sensing material, achieving extremely sensitive detection with LODs in the zeptomolar range. Zhi et al. (2014) showed detection of Hepatitis B virus (HBV)-genotype in a microfluidic system capable of identifying as few as 10 copies/ml. Furthermore, Lian et al. (2012) showed a fully realized lab-on-a-chip solution (Fig. 10) for diagnosing acute myocardial infarction. Their system was capable of multiplexed detection of up to 16 different targets, using magnetic nanoparticles as tags, with LODs as low as 10 pg mL^{-1} for human derived proteins. Additionally, Fernandes et al. (2014) have shown the continuous detection of magnetically labeled *Streptococcus agalactiae* in raw milk through magnetoresistive cytometry.

Regardless of the high sensitivity of the magnetoresistive sensors, their use in biosensing is so far quite limited, with the need for labeling of analytes possibly playing a major part. Compared to many of the other possible detection methods available for biosensors, the magnetoresistive sensors require a relatively complex protocol for detection.

17. Hall-sensors

Cheaper and more tolerant to high magnetic fields, but generally regarded as less sensitive (Popovic et al., 2002), the Hall-sensors offer a potentially mass producible alternative to the magnetoresistive sensors. Recent applications are few but indeed in much similar fields as what was described for the magnetoresistive sensors above. Rizzi et al. (2014) have shown detection of specific point mutations in the human beta globin (HBB) gene with LOD as low as 160 pM using a planar Hall effect bridge (PHEB) sensor. Using the same basic principle the sensor was later adapted for real time measurements of DNA-melting through temperature control of the chip (Rizzi et al., 2015). The Hall-sensors have also seen use in cytometry (Issadore et al., 2012) being able to detect labeled mammalian cells in whole blood. The same study even demonstrated possible differentiation between distinct cell types through labels with varied magnetization properties, tailoring them for specific cell membrane markers.

18. Conclusions and future perspectives

This review has attempted to offer readers an overview of recent examples of lab-on-a-chip solutions for biosensing applications. A number of tables are intended to provide the main salient features and thus allow readers to dive into relevant references for further study. Given the extreme variety in sensor designs, only amplified by combining them with a wealth of different microfluidic channel layouts, comparison between different realizations would be complex and offer little benefit to the reader. Many solutions presented in the literature are still very much at the proof-of-concept state, but it is also already more than obvious that there is enormous potential in bringing lab-on-a-chip's sample

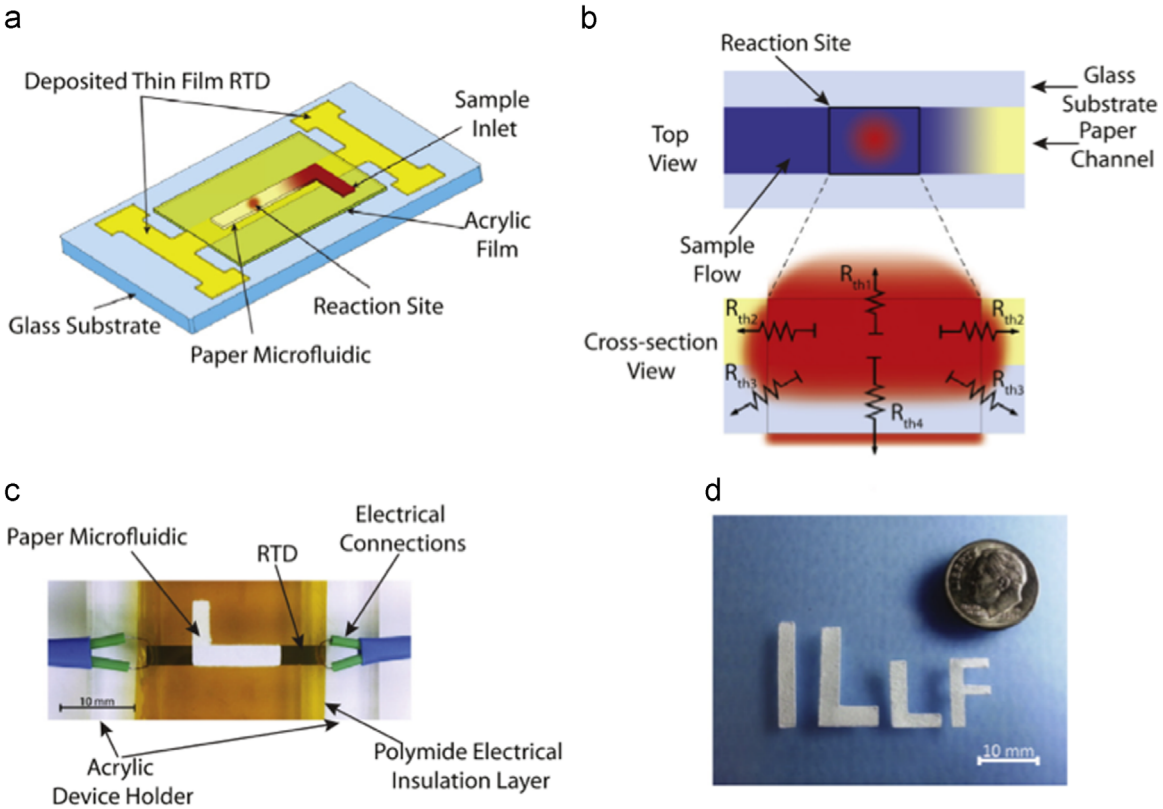

Fig. 9. (a) Overview of the paper-based device, (b) top view and cross-sectional view of the reaction site and heat transfer with the thermal resistance equivalent model, (c) fabricated paper-based microfluidic device with calorimetric detection, (d) knife plotter cut paper strips as a reaction substrate and a microfluidic channel. Reprinted with permission from Davaji and Lee (2014).

Table 6
Summary of recent studies utilizing magnetic biosensing in microfluidic applications.

Analyte or detected mechanism	Biological recognition element	Limit of detection (LOD)	Microfluidic chip feature	Reference
Magnetoresistance				
Multiple targets (antibody-biotin/streptavidin-magnetic bead sandwich)	Antibody	10 pg mL^{-1} Troponin I (419 zM[a])	Lab-on-a-chip solution with integrated storage wells; automatic control of protocol: analyte injection, antibody injection, wash, magnetic nanoparticle injection, and wash	Lian et al. (2012)
Biotin-HBV-genotype (streptavidin-magnetic beads)	DNA-probe	10 copies mL^{-1} (~17 zM[a])	PDMS/glass flow cell with GMR sensor.	Zhi et al. (2014)
Streptococcus agalactiae	Antibody- protein A-magnetic bead	Single bacteria	[b]PDMS/silicon flow cytometry cell with spin-valve sensor	Fernandes et al. (2014)
Hall-effect				
Biotin-human HBB-genotype (streptavidin-magnetic beads)	DNA-probe	156 pM	PMMA flow cell with PHEB sensor	Rizzi et al. (2014)
DNA-melting[c]	DNA-probe	N/A	PMMA flow cell with PHEB sensor	Rizzi et al. (2015)
Mammalian cells	Antibody-TCO-Tz-magnetic bead	Single cell	[b]PDMS/PHEMT-substrate flow cell with μHD sensor	Issadore et al. (2012)

Abbreviations used: hepatitis B virus (HBV), polydimethylsiloxane (PDMS), giant magnetoresistance (GMR), hemoglobin subunit beta (HBB), poly(methyl methacrylate) (PMMA), planar Hall-effect bridge (PHEB), transcyclooctene (TCO), 1,2,4,5-tetrazine (Tz), pseudomorphic high-electron mobility transistor (PHEMT), micro-Hall detector (mHD).

[a] Conversion by author.
[b] Continuous detection.
[c] Same detection mechanism as previously described (Rizzi et al. 2014).

preparation capabilities together with advanced biosensor designs. The enormous advantages of being able to pre-process sample solutions using microfluidics (e.g., cleaning them from interfering species, increasing the concentration of low abundant proteins, or labeling or tagging molecules to increase selectivity in the sensing step) will only broaden the application areas for lab-on-a-chip/biosensor systems and also relax some of the stringent requirements under which biosensors so far must be operated. Still, inherent challenges of biosensors stemming from the relative costliness of the sensing material and its susceptibility to fouling, and the resulting limited lifetime, will have to remain a focus of future research. One way forward here is clearly by finding or designing improved biological recognition elements, such as, e.g., aptamers or locked nucleic acids (LNA). The other main focus will be on bringing in materials that potentially can perform several important functions, such as provide structural support, be part of the transduction chain, and avoid fouling and disruption of the biorecognition process. Paradoxically, very novel materials such as graphene and other nanomaterials, and tailor-made (conductive) polymers may play a pivotal role here alongside materials already known for a long time, such as, e.g., paper. The number of publications on lab-on-a-chip/biosensor systems will certainly keep on increasing in the coming years and thus mirror the stormy development of this field. Substantial impact is to be expected in several life science disciplines, from point-of-care diagnostics, and food quality and environmental studies, to understanding and developing new drug candidates for personalized therapeutics.

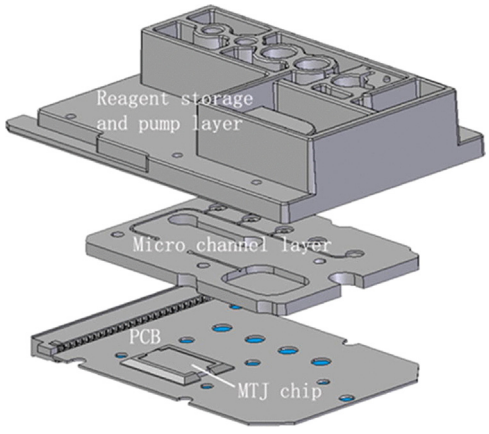

Fig. 10. Schematic of the lab-on-a-chip solution by Lian et al. (2012) for diagnosis of myocardial infarction. The bottom layer consists of a printed circuit board (PCB) and a magnetic tunnel junction (MTJ) sensor chip with immobilized antibodies. Reprinted with permission from Lian et al. (2012).

Acknowledgments

Authors JPL and AJ acknowledge funding from the Danish Council for Independent Research – Technology and Production (Grant no. DFF- 4005-00341). Author S.S. acknowledges funding from Denmark's Advanced Technology Foundation (Grant no. 144-2013-6).

References

Ali, M.A., Solanki, P.R., Patel, M.K., Dhayani, H., Agrawal, V.V., John, R., Malhotra, B.D., 2013. Nanoscale 5, 2883–2891.
Ali, M.A., Solanki, P.R., Srivastava, S., Singh, S., Agrawal, V.V., John, R., Malhotra, B.D., 2015. ACS Appl. Mater. Interfaces 7, 5837–5846.
Ali, M.A., Srivastava, S., Mondal, K., Chavhan, P.M., Agrawal, V.V., John, R., Sharma, A., Malhotra, B.D., 2014. Nanoscale 6, 13958–13969.
Alodhayb, A., Brown, N., Rahman, S.M.S., Harrigan, R., Beaulieu, L.Y., 2013. Appl. Phys. Lett. 102, 173106.
Angus, S.V., Kwon, H.-J., Yoon, J.-Y., 2012. J. Environ. Monit. 14, 3295–3304.
Arlett, J.L., Myers, E.B., Roukes, M.L., 2011. Nat. Nanotechnol. 6, 203–215.
Bache, M., Bosco, F.G., Brøgger, A.L., Frøhling, K.B., Alstrøm, T.S., Hwu, E.-T., Chen, C.-H., Eugen-Olsen, J., Hwang, I.-S., Boisen, A., 2013. Nanotechnology 24, 444011.
Bäcker, M., Rakowski, D., Poghossian, A., Biselli, M., Wagner, P., Schöning, M.J., 2013. Journal of Biotechnology. In: Proceedings of Biotech 2011 Conference—Sensor Technology and Process Analytics, vol. 163, pp. 371–376.
Ben-Yoav, H., Dykstra, P.H., Bentley, W.E., Ghodssi, R., 2012. Biosens. Bioelectron. 38, 114–120.
Ben-Yoav, H., Dykstra, P.H., Bentley, W.E., Ghodssi, R., 2015. Biosens. Bioelectron. 64, 579–585.
Besse, P.-A., Boero, G., Demierre, M., Pott, V., Popovic, R., 2002. Appl. Phys. Lett. 80, 4199–4201.
Bettazzi, F., Hamid-Asl, E., Esposito, C.L., Quintavalle, C., Formisano, N., Laschi, S., Catuogno, S., Iaboni, M., Marrazza, G., Mascini, M., Cerchia, L., De Franciscis, V., Condorelli, G., Palchetti, I., 2013. Anal. Bioanal. Chem. 405, 1025–1034.
Björk, P., Afrasiabi, R., Jokilaakso, N., Chen, S., Dev, A., Salter, M., Zhang, S.-L., Karlström, A.E., Linnros, J., 2014. Silicon nanowires/nanoribbons for label-free electrical detection of biomolecules. In: Proceedings of the 1st International

Seminar on Industrial Innovation in Electrochemistry. Editora Edgard Blücher, São Paulo, pp. 23–28.
Bog, U., Laue, T., Grossmann, T., Beck, T., Wienhold, T., Richter, B., Hirtz, M., Fuchs, H., Kalt, H., Mappes, T., 2013. Lab Chip 13, 2701–2707.
Borisov, S.M., Wolfbeis, O.S., 2008. Chem. Rev. 108, 423–461.
Bosco, F.G., Bache, M., Yang, J., Chen, C.H., Hwu, E.-T., Lin, Q., Boisen, A., 2013. Sens. Actuators Phys. 195, 154–159.
Bunde, R.L., Jarvi, E.J., Rosentreter, J.J., 1998. Talanta 46, 1223–1236.
Bunyakul, N., Baeumner, A.J., 2014. Sensors 15, 547–564.
Bunyakul, N., Promptmas, C., Baeumner, A.J., 2014. Anal. Bioanal. Chem., 1–10.
Cao, L., Cheng, L., Zhang, Z., Wang, Y., Zhang, X., Chen, H., Liu, B., Zhang, S., Kong, J., 2012. Lab Chip 12, 4864–4869.
Cerqueira, M.R.F., Grasseschi, D., Matos, R.C., Angnes, L., 2014. Talanta 126, 20–26.
Chen, D., Wang, J.J., Xu, Y., Liu, W.H., Wang, P., 2013. Electron. Lett. 49, 924–925.
Chen, J., Liu, Y., Ye, T., Xiang, X., Ji, X., He, Z., 2015a. Sens. Actuators B: Chem. 215, 206–214.
Chen, P., Chung, M.T., McHugh, W., Nidetz, R., Li, Y., Fu, J., Cornell, T.T., Shanley, T.P., Kurabayashi, K., 2015b. ACS Nano 9, 4173–4181.
Chiesa, M., Cardenas, P.P., Otón, F., Martinez, J., Mas-Torrent, M., Garcia, F., Alonso, J.C., Rovira, C., Garcia, R., 2012. Nano Lett. 12, 1275–1281.
Chung, J., Kang, J.S., Jurng, J.S., Jung, J.H., Kim, B.C., 2015. Biosens. Bioelectron. 67, 303–308.
Chun, H.J., Park, Y.M., Han, Y.D., Jang, Y.H., Yoon, H.C., 2014. BioChip J. 8, 218–226.
Cocovi-Solberg, D.J., Miró, M., Cerdà, V., Pokrzywnicka, M., Tymecki, Ł., Koncki, R., 2012. Talanta 96, 113–120.
Cohen, N., Sabhachandani, P., Golberg, A., Konry, T., 2015. Biosens. Bioelectron. 66, 454–460.
Comina, G., Suska, A., Filippini, D., 2015. Angew. Chem. Int. Ed. 54, 8708–8712.
Damhorst, G.L., Smith, C.E., Salm, E.M., Sobieraj, M.M., Ni, H., Kong, H., Bashir, R., 2013. Biomed. Microdevices 15, 895–905.
Daprà, J., Lauridsen, L.H., Nielsen, A.T., Rozlosnik, N., 2013. Biosens. Bioelectron 43, 315–320.
Date, Y., Terakado, S., Sasaki, K., Aota, A., Matsumoto, N., Shiku, H., Ino, K., Watanabe, Y., Matsue, T., Ohmura, N., 2012. Biosens. Bioelectron. 33, 106–112.
Davaji, B., Lee, C.H., 2014. Biosens. Bioelectron. 59, 120–126.
De, A., van Nieuwkasteele, J., Carlen, E.T., van den Berg, A., 2013. Real-time measurements of PNA:DNA hybridization kinetics with silicon nanowire biosensors. In: Proceedings of 2013 Transducers & Eurosensors XXVII: The 17th International Conference on Solid-State Sensors, Actuators and Microsystems. pp. 2795–2798.
De, A., Sparreboom, W., van den Berg, A., Carlen, E.T., 2014. Biomicrofluidics 8, 054119.
Dong, W., Luo, J., He, H., Jiang, L., 2013. Int. J. Nanomed. 8, 221–232.
Donolato, M., Antunes, P., de la Torre, T.Z.G., Hwu, E.-T., Chen, C.-H., Burger, R., Rizzi, G., Bosco, F.G., Strømme, M., Boisen, A., Hansen, M.F., 2015. Biosens. Bioelectron. 67, 649–655.
Duval, D., González-Guerrero, A.B., Dante, S., Osmond, J., Monge, R., Fernández, L.J., Zinoviev, K.E., Domínguez, C., Lechuga, L.M., 2012. Lab Chip 12, 1987–1994.
Escobedo, C., Chou, Y.-W., Rahman, M., Duan, X., Gordon, R., Sinton, D., Brolo, A.G., Ferreira, J., 2013. Analyst 138, 1450–1458.
Estevez, M.-C., Otte, M.A., Sepulveda, B., Lechuga, L.M., 2014. Anal. Chim. Acta 806, 55–73.
Fan, X., White, I.M., Shopova, S.I., Zhu, H., Suter, J.D., Sun, Y., 2008. Anal. Chim. Acta 620, 8–26.
Ferguson, B.S., Hoggarth, D.A., Maliniak, D., Ploense, K., White, R.J., Woodward, N., Hsieh, K., Bonham, A.J., Eisenstein, M., Kippin, T.E., 2013. Sci. Transl. Med. 5, 213ra165.
Fernandes, A.C., Duarte, C.M., Cardoso, F.A., Bexiga, R., Cardoso, S., Freitas, P.P., 2014. Sensors 14, 15496–15524.
Ferrie, A.M., Wang, C., Deng, H., Fang, Y., 2013. Integr. Biol. 5, 1253–1261.
Ferrier, D.C., Shaver, M.P., Hands, P.J.W., 2015. Biosens. Bioelectron. 68, 798–810.
Gammoudi, I., Raimbault, V., Tarbague, H., Moroté, F., Grauby-Heywang, C., Othmane, A., Kalfat, R., Moynet, D., Rebière, D., Dejous, C., Cohen-Bouhacina, T., 2014. Sens. Actuators B: Chem. 198, 278–284.
Ge, X., Asiri, A.M., Du, D., Wen, W., Wang, S., Lin, Y., 2014. TrAC Trends Anal. Chem. 58, 31–39.
Ghosh Dastider, S., Barizuddin, S., Yuksek, N.S., Dweik, M., Almasri, M.F., 2015. J. Sens., e293461.
Grego, S., Gilchrist, K.H., Carlson, J.B., Stoner, B.R., 2012. Sens. Actuators B: Chem. 161, 721–727.
Grieshaber, D., MacKenzie, R., Vörös, J., Reimhult, E., 2008. Sensors 8, 1400–1458.
Guo, L., Yin, Y., Huang, R., Qiu, B., Lin, Z., Yang, H.-H., Li, J., Chen, G., 2012. Lab Chip 12, 3901–3906.
Gu, S., Lu, Y., Ding, Y., Li, L., Song, H., Wang, J., Wu, Q., 2014. Biosens. Bioelectron. 55, 106–112.
Han, D., Kim, Y.-R., Kang, C.M., Chung, T.D., 2014. Anal. Chem. 86, 5991–5998.
Han, K.N., Li, C.A., Seong, G.H., 2013. Annu. Rev. Anal. Chem. 6, 119–141.
Han, S.W., Jang, E., Koh, W.-G., 2015. Sens. Actuators B: Chem. 209, 242–251.
Hao, H.-C., Chang, H.-Y., Wang, T.-P., Yao, D.-J., 2013. J. Lab. Autom. 18, 69–76.
Hemmilä, S., Gao, A., Lu, N., Li, T., Wang, Y., Kallio, P., 2014. Microsyst. Technol. 21, 571–580.
He, P., Oncescu, V., Lee, S., Choi, I., Erickson, D., 2013. Anal. Chim. Acta 759, 74–80.
Hervás, M., López, M.A., Escarpa, A., 2012. TrAC Trends Anal. Chem. 31, 109–128.
Hofmann, U., Michaelis, S., Winckler, T., Wegener, J., Feller, K.-H., 2013. Biosens. Bioelectron. 39, 156–162.
Holzinger, M., Le Goff, A., Cosnier, S., 2014. Front. Chem. 2, 63.
Hong, C.-C., Lin, C.-C., Hong, C.-L., Chang, P.-H., 2012. Biomed. Microdevices 14, 435–441.
Horak, J., Dincer, C., Bakirci, H., Urban, G., 2014. Sens. Actuators B: Chem. 191, 813–820.
Ispas, C.R., Crivat, G., Andreescu, S., 2012. Anal. Lett. 45, 168–186.
Issadore, D., Chung, J., Shao, H., Liong, M., Ghazani, A.A., Castro, C.M., Weissleder, R., Lee, H., 2012. Sci. Transl. Med. 4, 141ra92.
Itoh, D., Sassa, F., Nishi, T., Kani, Y., Murata, M., Suzuki, H., 2012. Sens. Actuators B: Chem. 171–172, 619–626.
Jang, E., Kim, S., Koh, W.-G., 2012. Biosens. Bioelectron. 31, 529–536.
Janz, S., Xu, D.-X., Vachon, M., Sabourin, N., Cheben, P., McIntosh, H., Ding, H., Wang, S., Schmid, J.H., Delâge, A., Lapointe, J., Densmore, A., Ma, R., Sinclair, W., Logan, S.M., MacKenzie, R., Liu, Q.Y., Zhang, D., Lopinski, G., Mozenson, O., Gilmour, M., Tabor, H., 2013. Opt. Express 21, 4623.
Jiang, Y., Wang, H., Li, S., Wen, W., 2014. Sensors 14, 6952–6964.
Jin, S., Dai, M., He, F., Wang, Y., Ye, B.-C., Nugen, S.R., 2012. Microsyst. Technol. 18, 731–737.
Kelley, S.O., Mirkin, C.A., Walt, D.R., Ismagilov, R.F., Toner, M., Sargent, E.H., 2014. Nat. Nanotechnol. 9, 969–980.
Kim, G., Moon, J.-H., Moh, C.-Y., Lim, J.-G., 2015. Biosens. Bioelectron. 67, 243–247.
Kim, J., Elsnab, J., Gehrke, C., Li, J., Gale, B.K., 2013a. Sens. Actuators B: Chem. 185, 370–376.
Kimmel, D.W., LeBlanc, G., Meschievitz, M.E., Cliffel, D.E., 2012. Anal. Chem. 84, 685–707.
Kim, M., Kim, T., 2014. Sens. Actuators B: Chem. 202, 1229–1236.
Kim, T.-H., Abi-Samra, K., Sunkara, V., Park, D.-K., Amasia, M., Kim, N., Kim, J., Kim, H., Madou, M., Cho, Y.-K., 2013b. Lab Chip 13, 3747–3754.
Krupin, O., Asiri, H., Wang, C., Tait, R.N., Berini, P., 2013. Opt. Express 21, 698.
Kumeria, T., Kurkuri, M.D., Diener, K.R., Parkinson, L., Losic, D., 2012. Biosens. Bioelectron. 35, 167–173.
Lafleur, J.P., Senkbeil, S., Jensen, T.G., Kutter, J.P., 2012. Lab Chip 12, 4651–4656.
Lafleur, J.P., Senkbeil, S., Novotny, J., Nys, G., Bøgelund, N., Rand, K.D., Foret, F., Kutter, J.P., 2015. Lab Chip 15, 2162–2172.
Lee, I., Luo, X., Huang, J., Cui, X.T., Yun, M., 2012. Biosensors 2, 205–220.
Lee, S.-W., Saraf, R.F., 2014. Biosens. Bioelectron. 57, 41–47.
Lian, J., Chen, S., Qiu, Y., Zhang, S., Shi, S., Gao, Y., 2012. J. Appl. Phys. 111, 07B315.
Li, B., Li, L., Guan, A., Dong, Q., Ruan, K., Hu, R., Li, Z., 2014a. Lab Chip 14, 4085–4092.
Li, M., Wang, Y., Zhang, Y., Yu, J., Ge, S., Yan, M., 2014b. Biosens. Bioelectron. 59, 307–313.
Lin, C.-L., Chang, W.-H., Wang, C.-H., Lee, C.-H., Chen, T.-Y., Jan, F.-J., Lee, G.-B., 2015. Biosens. Bioelectron. 63, 572–579.
Lin, F., 2014. Analyst 139, 2890–2895.
Lisdat, F., Schäfer, D., 2008. Anal. Bioanal. Chem. 391, 1555–1567.
Liu, F., Piao, Y., Choi, J.S., Seo, T.S., 2013. Biosens. Bioelectron. 50, 387–392.
Liu, F., Zhang, C., 2015. Sens. Actuators B: Chem. 209, 399–406.
Liu, H., Xiang, Y., Lu, Y., Crooks, R.M., 2012a. Angew. Chem. Int. Ed. 51, 6925–6928.
Liu, Y., Kwa, T., Revzin, A., 2012b. Biomaterials 33, 7347–7355.
Liu, Y., Liu, Y., Matharu, Z., Rahimian, A., Revzin, A., 2015. Biosens. Bioelectron. 64, 43–50.
Liu, Y., Matharu, Z., Howland, M.C., Revzin, A., Simonian, A.L., 2012c. Anal. Bioanal. Chem. 404, 1181–1196.
Llandro, J., Palfreyman, J.J., Ionescu, A., Barnes, C.H.W., 2010. Med. Biol. Eng. Comput. 48, 977–998.
Long, F., Zhu, A., Zhou, X., Wang, H., Zhao, Z., Liu, L., Shi, H., 2014. Biosens. Bioelectron. 55, 19–25.
Longo, G., Alonso-Sarduy, L., Rio, L.M., Bizzini, A., Trampuz, A., Notz, J., Dietler, G., Kasas, S., 2013. Nat. Nanotechnol. 8, 522–526.
Lynn, N.S., Bocková, M., Adam, P., Homola, J., 2015. Anal. Chem. 87, 5524–5530.
Lynn, N.S., Homola, J., 2015. Anal. Chem. 87, 5516–5523.
Lynn, N.S., Šípová, H., Adam, P., Homola, J., 2013. Lab Chip 13, 1413–1421.
Malic, L., Morton, K., Clime, L., Veres, T., 2013. Lab Chip 13, 798–810.
Manesse, M., Phillips, A.F., LaFratta, C.N., Palacios, M.A., Hayman, R.B., Walt, D.R., 2013. Lab Chip 13, 2153–2160.
Mariotti, S., 2011. Physiology of the Hypothalamic-Pituitary Thyroidal System [WWW Document]. Thyroid Disease Manager. URL http://www.thyroidmanager.org/chapter/physiology-of-the-hypothalmic-pituitary-thyroidal-system/ (accessed 5.19.15).
Marty, M.T., Sloan, C.D.K., Bailey, R.C., Sligar, S.G., 2012. Anal. Chem. 84, 5556–5564.
Matatagui, D., Moynet, D., Fernández, M.J., Fontecha, J., Esquivel, J.P., Gràcia, I., Cané, C., Déjous, C., Rebière, D., Santos, J.P., Horrillo, M.C., 2013. Sens. Actuators B: Chem. 185, 218–224.
Matharu, Z., Enomoto, J., Revzin, A., 2013. Anal. Chem. 85, 932–939.
Matharu, Z., Patel, D., Gao, Y., Haque, A., Zhou, Q., Revzin, A., 2014. Anal. Chem. 86, 8865–8872.
Mirasoli, M., Bonvicini, F., Dolci, L.S., Zangheri, M., Gallinella, G., Roda, A., 2012. Anal. Bioanal. Chem. 405, 1139–1143.
Mohammed, M.I., Desmulliez, M.P.Y., 2014. Biosens. Bioelectron. 61, 478–484.
Moral-Vico, J., Barallat, J., Abad, L., Olivé-Monllau, R., Muñoz-Pascual, F.X., Galán Ortega, A., del Campo, F.J., Baldrich, E., 2015. Biosens. Bioelectron. 69, 328–336.
Morant-Miñana, M.C., Elizalde, J., 2015. Biosens. Bioelectron. 70, 491–497.
Muzyka, K., 2014. Biosens. Bioelectron. 54, 393–407.
Myers, F.B., Lee, L.P., 2008. Lab Chip 8, 2015–2031.
Novo, P., Chu, V., Conde, J.P., 2014. Biosens. Bioelectron. 57, 284–291.
O'Sullivan, C.K., Guilbault, G.G., 1999. Biosens. Bioelectron. 14, 663–670.
Ölcer, Z., Esen, E., Ersoy, A., Budak, S., Sever Kaya, D., Yağmur Gök, M., Barut, S., Üstek, D., Uludag, Y., 2015. Biosens. Bioelectron. 70, 426–432.

Park, J., Karsten, S.L., Nishida, S., Kawakatsu, H., Fujita, H., 2012. Lab Chip 12, 4115–4119.
Patolsky, F., Timko, B.P., Zheng, G., Lieber, C.M., 2007. MRS Bull 32, 142–149.
Peng, H.-I., Strohsahl, C.M., Miller, B.L., 2012. Lab Chip: Miniat. Chem. Biol. 12, 1089–1093.
Picher, M.M., Küpcü, S., Huang, C.-J., Dostalek, J., Pum, D., Sleytr, U.B., Ertl, P., 2013. Lab Chip 13, 1780–1789.
Popovic, R.S., Drljaca, P.M., Schott, C., 2002. Bridging the gap between AMR, GMR, and Hall magnetic sensors. In: 23rd International Conference on Microelectronics (MIEL 2002), vol. 1, pp. 55–58.
Porwal, A., Narsude, M., Rao, V.R., Mukherji, S., 2002. IETE Tech. Rev. 19, 257–267.
Ramanathan, K., Bangar, M.A., Yun, M., Chen, W., Myung, N.V., Mulchandani, A., 2005. J. Am. Chem. Soc. 127, 496–497.
Rattanarat, P., Teengam, P., Siangproh, W., Ishimatsu, R., Nakano, K., Chailapakul, O., Imato, T., 2015. Electroanalysis 27, 703–712.
van Reenen, A., de Jong, A.M., den Toonder, J.M.J., Prins, M.W.J., 2014. Lab Chip 14, 1966–1986.
Regiart, M., Fernández-Baldo, M.A., Spotorno, V.G., Bertolino, F.A., Raba, J., 2013. Biosens. Bioelectron. 41, 211–217.
Rizzi, G., Østerberg, F.W., Henriksen, A.D., Dufva, M., Hansen, M.F., 2015. Journal of Magnetism and Magnetic Materials. In: Proceedings of the 10th International Conference on the Scientific and Clinical Applications of Magnetic Carriers. 10–14 June 2014, Dresden, Germany 380, pp. 215–220.
Rizzi, G., Westergaard Østerberg, F., Dufva, M., Fougt Hansen, M., 2014. Biosens. Bioelectron. 52, 445–451.
Rocha-Santos, T.A.P., 2014. TrAC: Trends Anal. Chem. 62, 28–36.
Roda, A., Cevenini, L., Borg, S., Michelini, E., Calabretta, M.M., Schüler, D., 2013. Lab Chip 13, 4881–4889.
SadAbadi, H., Badilescu, S., Packirisamy, M., Wüthrich, R., 2013. Biosens. Bioelectron. 44, 77–84.
Salleh, M.H.M., Glidle, A., Sorel, M., Reboud, J., Cooper, J.M., 2013. Chem. Commun. 49, 3095–3097.
Sang, S., Witte, H., 2010. Biosens. Bioelectron. 25, 2420–2424.
Sang, S., Zhao, Y., Zhang, W., Li, P., Hu, J., Li, G., 2014. Biosens. Bioelectron. 51, 124–135.
Seefeld, T.H., Halpern, A.R., Corn, R.M., 2012. J. Am. Chem. Soc. 134, 12358–12361.
Seenivasan, R., Maddodi, N., Setaluri, V., Gunasekaran, S., 2015. Biosens. Bioelectron. 68, 508–515.
Seia, M.A., Pereira, S.V., Fernández-Baldo, M.A., Vito, I.E.D., Raba, J., Messina, G.A., 2014. Anal. Bioanal. Chem. 406, 4677–4684.
Şen, M., Ino, K., Shiku, H., Matsue, T., 2012. Lab Chip 12, 4328–4335.
Shin, D.-S., Liu, Y., Gao, Y., Kwa, T., Matharu, Z., Revzin, A., 2013. Anal. Chem. 85, 220–227.
Sim, J.H., Kwak, Y.H., Choi, C.H., Paek, S.-H., Park, S.S., Seo, S., 2012. Sens. Actuators B: Chem. 173, 752–759.
Song, B., Pan, S., Tang, C., Li, D., Rusling, J.F., 2013. Anal. Chem. 85, 11061–11067.
Squires, T.M.T., Messinger, R.J.R., Manalis, S.R.S., 2008. Nat. Biotechnol. 26, 417–426.
Taitt, C.R., Anderson, G.P., Ligler, F.S., 2005. Biosens. Bioelectron. 20, 2470–2487.
Tamayo, J., Kosaka, P.M., Ruz, J.J., Paulo, Á.S., Calleja, M., 2013. Chem. Soc. Rev. 42, 1287–1311.
Tan, S.N., Ge, L., Tan, H.Y., Loke, W.K., Gao, J., Wang, W., 2012. Anal. Chem. 84, 10071–10076.
Trantum, J.R., Baglia, M.L., Eagleton, Z.E., Mernaugh, R.L., Haselton, F.R., 2013. Lab Chip 14, 315–324.
Truffer, F., Buffi, N., Merulla, D., Beggah, S., Lintel, H. van, Renaud, P., Meer, J.R. van der, Geiser, M., 2014. Rev. Sci. Instrum. 85, 015120.
Tsai, H.-F., Tsai, Y.-C., Yagur-Kroll, S., Palevsky, N., Belkin, S., Cheng, J.-Y., 2015. Lab Chip 15, 1472–1480.
Vabbina, P.K., Kaushik, A., Pokhrel, N., Bhansali, S., Pala, N., 2015. Biosens. Bioelectron. 63, 124–130.
Varma, S., Voldman, J., 2015. Lab Chip 15, 1563–1573.
Vasudev, A., Kaushik, A., Tomizawa, Y., Norena, N., Bhansali, S., 2013. Sens. Actuators B: Chem. 182, 139–146.
Voinova, M.V., 2009. J. Sens. 2009, e943125.
Wang, J., 2006. Analytical Electrochemistry. John Wiley & Sons, Hoboken, USA.
Wang, J., Aki, M., Onoshima, D., Arinaga, K., Kaji, N., Tokeshi, M., Fujita, S., Yokoyama, N., Baba, Y., 2014a. Biosens. Bioelectron. 51, 280–285.
Wang, S.X., Li, G., 2008. IEEE Trans. Magn. 44, 1687–1702.
Wang, X., Flueckiger, J., Schmidt, S., Grist, S., Fard, S.T., Kirk, J., Doerfler, M., Cheung, K.C., Ratner, D.M., Chrostowski, L., 2013a. J. Biophotonics 6, 821–828.
Wang, X., Zhan, S., Huang, Z., Hong, X., 2013b. Instrum. Sci. Technol. 41, 574–607.
Wang, Y., Ye, Z., Ping, J., Jing, S., Ying, Y., 2014b. Biosens. Bioelectron. 59, 106–111.
Weng, X., Zhao, W., Neethirajan, S., Duffield, T., 2015. J. Nanobiotechnol. 13, 13.
Wang, Z., Chen, J., Fan, Y., Wang, W., Fu, F., 2013c. Microfluid. Nanofluid. 14, 145–152.
Xiang, X., Chen, L., Zhuang, Q., Ji, X., He, Z., 2012a. Biosens. Bioelectron. 32, 43–49.
Xiang, X., Luo, M., Shi, L., Ji, X., He, Z., 2012b. Anal. Chim. Acta 751, 155–160.
Xu, T., Yu, H., Xu, P., Xu, W., Chen, W., Chen, C., Li, X., 2014. Lab Chip 14, 1206–1214.
Yakovleva, M., Bhand, S., Danielsson, B., 2013. Anal. Chim. Acta 766, 1–12.
Yen, Y.-K., Lai, Y.-C., Hong, W.-T., Pheanpanitporn, Y., Chen, C.-S., Huang, L.-S., 2013. Sensors 13, 9653–9668.
Ye, W.W., Shi, J.Y., Chan, C.Y., Xiao, L.D., Yang, M., 2013. Nanoporous alumina membrane and nanoparticle based microfluidic sensing platform for direct DNA detection. In: Proceedings of 2013 Transducers & Eurosensors XXVII: The 17th International Conference on Solid-State Sensors, Actuators and Microsystems. pp. 1255–1258.
Yin, T.-I., Zhao, Y., Horak, J., Bakirci, H., Liao, H.-H., Tsai, H.-H., Juang, Y.-Z., Urban, G., 2013. Lab Chip 13, 834–842.
Yoon, Y.-J., Li, K.H.H., Low, Y.Z., Yoon, J., Ng, S.H., 2014. Sens. Actuators B: Chem. 198, 233–238.
Zhang, B., Feldman, A., Wang, Q., 2013. Sens. Actuators B: Chem. 186, 597–602.
Zhang, G.-J., Ning, Y., 2012. Anal. Chim. Acta 749, 1–15.
Zhang, H., Hu, X., Fu, X., 2014. Biosens. Bioelectron. 57, 22–29.
Zhang, Y., Zuo, P., Ye, B.-C., 2015. Biosens. Bioelectron. 68, 14–19.
Zhao, W.-W., Xu, J.-J., Chen, H.-Y., 2014. Chem. Soc. Rev. 44, 729–741.
Zhi, X., Deng, M., Yang, H., Gao, G., Wang, K., Fu, H., Zhang, Y., Chen, D., Cui, D., 2014. Biosens. Bioelectron. 54, 372–377.
Zhou, J., Ellis, A.V., Kobus, H., Voelcker, N.H., 2012. Anal. Chim. Acta 719, 76–81.
Zhu, X., Xu, L., Wu, T., Xu, A., Zhao, M., Liu, S., 2014. Biosens. Bioelectron. 55, 438–445.
Zitka, O., Krizkova, S., Skalickova, S., Dospivova, D., Adam, V., Kizek, R., 2013. Electrophoresis 34, 2120–2128.
Zuzuarregui, A., Souto, D., Pérez-Lorenzo, E., Arizti, F., Sánchez-Gómez, S., Martínez de Tejada, G., Brandenburg, K., Arana, S., Mujika, M., 2014. Analyst 140, 654–660.